

ABSTRACT

RAMACHANDRAN, ARAVIND. Global Features of Flame Stabilization in Turbulent Non-premixed Jet Flames in Vitiated Coflow. (Under the direction of Dr. Venkateswaran Narayanaswamy.)

Turbulent combustion of non-premixed methane jet issuing into a vitiated coflow is studied in the Turbulent Shear Flow Laboratory at North Carolina State University. Luminosity imaging was performed to delineate the dominant motions executed by the turbulent flame. Three distinct modes – a relatively stable flame base (Mode A), flame executing blowout motion (Mode B) and a flame executing blowout motion that is re-anchored by autoignition kernels (Mode C) – are identified. The role of autoignition in stabilizing the Mode A motions of the flames was assessed. Chemical kinetic simulations were performed for homogeneous CH_4/Air mixtures over a range of mixture temperatures and oxygen mole fractions. Ignition delay time and evolution of OH and CH_2O radicals were observed. Global chemical time scales derived from flame liftoff height were compared against ignition time scales obtained from chemical kinetics. Under homogeneous situations, over a range of temperatures, the ignition delay times were found to be of comparable or smaller order of magnitude than the flow transit time corresponding to flame liftoff height of Mode A. At lower temperatures, it is expected that the role of autoignition would diminish. Statistics of the probability of occurrence of different flame modes was analyzed from the experimental data obtained across a matrix of test flame configurations where the coflow temperature, oxygen mole fraction of the coflow combustion products, and the fuel jet Reynolds number were varied. It was inferred from these studies that autoignition could play a significant role in the stabilization of turbulent jet flames at high coflow temperatures, but

the effect of turbulence could be crucial in determining the dominant stabilization mechanism at lower temperatures.

© Copyright 2015 Aravind Ramachandran
All Rights Reserved

Global Features of Flame Stabilization in Turbulent Non-premixed
Jet Flames in Vitiated Coflow

by
Aravind Ramachandran

A thesis submitted to the Graduate Faculty of
North Carolina State University
in partial fulfillment of the
requirements for the Degree of
Master of Science

Aerospace Engineering

Raleigh, North Carolina

2015

APPROVED BY:

Dr. Venkateswaran Narayanaswamy
Committee Chair

Dr. Kevin M. Lyons

Dr. Tiegang Fang

DEDICATION

To my good friends Calvin and Hobbes.

BIOGRAPHY

Aravind Ramachandran was born in Alappuzha (in the state of Kerala), India in 1990. He completed his B.E. in Mechanical Engineering from Sri Venkateswara College of Engineering, Anna University Chennai in 2012 and is pursuing a PhD in Aerospace Engineering at NC State.

ACKNOWLEDGMENTS

I would like to thank my family, friends, teachers, advisor and labmates for helping me achieve this.

TABLE OF CONTENTS

LIST OF TABLES	vii
LIST OF FIGURES	viii
1 INTRODUCTION.....	1
1.1 Lifted Flames	3
1.2 Stabilization of Conventional Lifted Flames	4
1.3 Stabilization of Lifted Jet Flames in High Temperature Environment	9
2 EXPERIMENTAL METHODS	15
2.1 Experimental Setup.....	15
2.1.1 Perforated Copper Plate (Flame Holder)	17
2.1.2 Ceramic Honeycomb Flow Conditioner	19
2.1.3 Flow Control System.....	20
2.1.4 Mixing Chamber	22
2.1.5 Fuel Jet.....	23
2.1.6 Exit Collar.....	24
2.1.7 Summary.....	25
2.2 Coflow Exit Conditions.....	26
2.3 Tests Performed.....	29
2.4 Image Acquisition and Processing.....	33
3 RESULTS AND DISCUSSION	36
3.1 Global Observations of the Lifted Jet Flames	36
3.1.1 Stable Flame Base (Mode A).....	37
3.1.2 Flame Blowout (Mode B).....	39
3.1.3 Autoignition Kernel Formation and Flame Re-anchor (Mode C).....	45
3.2 Contribution of Autoignition vs. Partial Premixing in Mode A Motions	48
3.2.1 Chemical Kinetics Results.....	50
3.3 Other Observations from Experiments.....	56
3.4 Influence of Aero/thermochemical Properties on Flame Stabilization	57
4 CONCLUSIONS	62
4.1 Concluding Remarks	62

4.2	Future Work.....	64
5	REFERENCES.....	66

LIST OF TABLES

Table 1: Test Matrix	30
-----------------------------------	-----------

LIST OF FIGURES

Figure 1: Schematic diagram of a lifted jet flame showing a temporally resolved flame base structure [1].....	3
Figure 2: Schematic diagram of the premixed flame base and trailing diffusion flame based on the description given by Vanquickenborne and Van Tiggelen. [6]	5
Figure 3: Illustration of the structure of a triple flame based on the illustration of Muñiz and Mungal [12].....	6
Figure 4: Illustration of a large scale structure influencing the base of a lifted flame based on the illustration by Kelman et al. [23].....	8
Figure 5: Schematic diagram of a burner with a lifted <i>CH4</i> jet flame in a vitiated coflow produced by <i>H2/Air</i> combustion. [25].....	9
Figure 6: Comparison of temporal evolution of liftoff height of a jet flame in vitiated coflow (left) vs cold coflow (right). [26].....	10
Figure 7: DNS mass fraction plot showing <i>HO2</i> radical buildup upstream of the flame base of an ethylene jet in a heated coflow. [28]	11
Figure 8: Schematic of the Experimental Setup.....	15
Figure 9: Copper Flame Holder Plate.....	17
Figure 10: Ceramic Flow Conditioner	20
Figure 11: Mixing chamber with the air-fuel mixture entering it tangentially.....	22
Figure 12: Fuel jet tube entering the burner through the bore-through connector	23
Figure 13: Steel Exit Collar.....	25

Figure 14: Thermocouple measurements 26

Figure 15: Radial temperature profile of the vitiated coflow. These measurements were taken for a coflow equivalence ratio of 0.5. The coflow adiabatic flame temperature for this case was 1475 K..... 28

Figure 16: Temporal evolution of flame liftoff height for two cases: 1) $\phi = 0.625, T_{co} = 1705$ K, jet exit height from coflow = 6.5” (165 mm) and 2) $\phi = 0.5, T_{co} = 1475$ K, jet exit height from coflow = 1.5” (38 mm) 31

Figure 17: Comparison of raw image obtained from camera and the contrast stretched image after processing using ImageJ 33

Figure 18: Flame luminosity image and the corresponding binary image of the flame edge..... 34

Figure 19: Time series of liftoff height for equivalence ratio of 0.625 at a Reynolds number of 4500. The coflow adiabatic temperature for this case is 1705 K. This time series shows the occurrence of the three flame modes..... 37

Figure 20: Image sequence demonstrating the lifted turbulent jet flame exhibiting Mode A. Low fluctuations of the flame base can be seen here. Flame stems are marked in image (a)..... 38

Figure 21: Image Sequence showing blowout of the jet flame, i.e., Mode B. The images shown here are of successive frames recorded at a rate of 60 frames per second. 41

Figure 22: Binary image sequence of Mode B, which clearly shows the extinction of a leading edge flame stem at the start of the blowout process. This binary image sequence corresponds to the sequence shown in Figure 21. 43

Figure 23: Image sequence illustrating the relight sequence of the jet flame succeeding an occurrence of blowout (Mode B). 45

Figure 24: Image sequence demonstrating the formation of ignition kernels and the subsequent re-anchoring of the lifted jet flame..... 47

Figure 25: Sample plot illustrating the evolution of temperature, *CH2O* mole fraction and *OH* mole fraction. This plot corresponds to the simulated case with a mixture temperature of 1700 K and *XO2* = 7.39%..... 50

Figure 26: Ignition delay time computed by Cantera for a range of oxygen mole fractions. The temperature of the homogeneous mixture was set at 1705 K..... 51

Figure 27: Logarithmic scale plot of ignition delay time of a homogeneous *CH4*/*Air* mixture at atmospheric pressure and *XO2*= 7.39% computed by Cantera for a range of starting fuel-oxidizer mixture temperatures. 52

Figure 28: Change in ignition delay time, maximum *OH* and *CH2O* mole fractions and *CH2O* peak time with mixture temperature, plotted for a homogeneous *CH4*/*Air* mixture at *XO2* = 7.39%. The *OH* mole fraction is scaled down by a factor of 10..... 54

Figure 29: Minima in maximum *CH2O* mole fraction observed at similar mixture temperature for three different values of *XO2* 55

Figure 30: Random Spots' regime observed at jet Reynolds number of 4500, coflow adiabatic flame temperature of 1475 K and at 4.26% *O2* mole fraction..... 57

Figure 31: Flame mode percentages compared for three cases: (a) $\Phi = 0.5$, $ReD = 4500$, (b) $\Phi = 0.575$, $ReD = 4500$, and (c) $\Phi = 0.575$, $ReD = 8000$ 58

Figure 32: Temporal evolution of temperature, CH_2O mole fraction and OH mole fraction (scaled down to match the peak in CH_2O) for a homogeneous CH_4/Air mixture at a starting temperature of 1475 K and $X_{O_2} = 9.98\%$ 60

Figure 33: Temporal evolution of temperature, CH_2O mole fraction and OH mole fraction (scaled down to match the peak in CH_2O) for a homogeneous CH_4/Air mixture at a starting temperature of 1615 K and $X_{O_2} = 8.42\%$ 59

1 INTRODUCTION

Ever since the discovery of fire, understanding its uses has fueled mankind's progress and propelled us to where we stand at present. Developing uses for the energy obtained from the combustion of fossil fuels has been key to technological advancements over the centuries. The development of every modern combustor – lean premixed burners, afterburners, gas turbines, homogeneous charge compression ignition (HCCI) engines, to name a few – has been the result of several years of research, and there is a wealth of ongoing experimental and computational research aimed towards improving our understanding of complex combustion phenomena. The impact of combustion has never diminished and it continues to be a phenomenon that plays a significant role in our daily lives – predominantly in transportation and energy. The combustion process has several benefits but fossil fuel combustion also brings with it some environmental hazards. Over the past quarter century, with a large increase in the volume of automobile production and the demand for energy, the attention of scientists, engineers and policymakers has been directed towards pollution. Therefore, from the age when the first combustion researcher confirmed that rubbing two stones to obtain a spark was a repeatable experiment, we have come a long way to the 21st century, where the focus is on goals such as minimizing pollutant emissions and maximizing combustion efficiency.

There has been significant impetus to develop clean combustion technologies that can cut emissions by over 50% before 2030. In particular, emphasis has been placed on low

temperature combustion with Exhaust Gas Recirculation (EGR), in which combustion products from the engine are recirculated into the combustion chamber to slow down the overall pollutant formation chemistry. This recirculation process results in the air in the combustion chamber getting *vitiated*, i.e., the oxidizer composition gets diluted by the addition of hot combustion products, reducing the amount of oxygen available for the combustion process. The applications of turbulent combustion in a vitiated environment reach across the realm of diesel engines, gas turbines, afterburners and industrial burners. In fact, the knowledge of stabilization and extinction of flames in an environment of combustion products could also be considered to be the key to containing and preventing the spread of wildfires and compartment fires. Also, turbulent flames that occur in boilers, gas turbines and elevated flares are lifted flames, i.e., the flames are not stabilized on a burner lip or any such physical surface. Thus, the benefits of understanding the stabilization mechanisms of lifted turbulent flames are substantial to the scientific community. This entails a detailed investigation of combustion of fuels in oxygen-parched conditions to understand the combustion phenomena that occur in clean combustors.

1.1 Lifted Flames

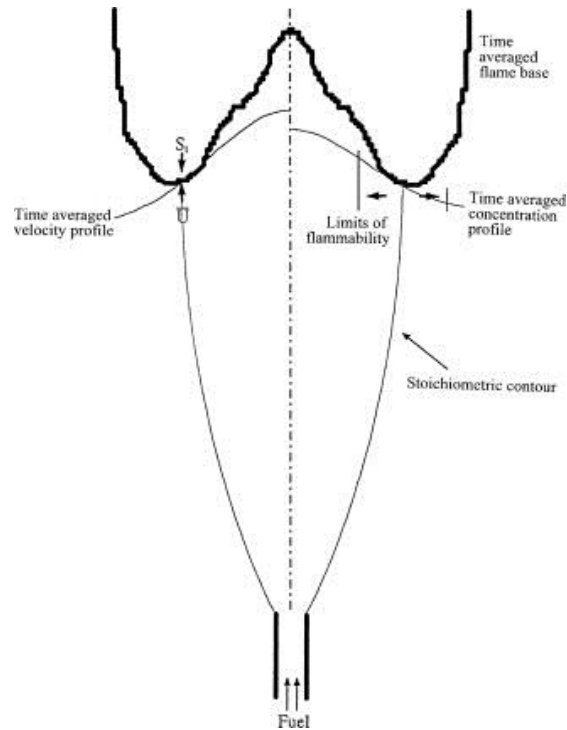


Figure 1: Schematic diagram of a lifted jet flame showing a temporally resolved flame base structure [1]

A canonical experimental configuration that has been used by combustion researchers over the years is that of a jet of fuel issuing into a coaxial flow (commonly referred to as ‘coflow’) of oxidizer, usually air, at a lower velocity than that of the fuel jet. Several examples of the early research in this configuration had the jet flame stabilized in an environment of quiescent air. The main purpose of adding a coaxial flow of air was to shield the jet from entrainment of ambient air and to ensure uniform aerothermochemical conditions of the coflow. Increasing the fuel jet velocity or the velocity of the coflowing air would result in a lifted flame. The laboratory lifted flame produced by this experimental configuration, as shown in Figure 1, is an invaluable tool for studying flame stabilization mechanisms. The

chief advantage of this configuration is that the complex fluid dynamics that occur in actual combustors is decoupled from the problem, thus allowing the researcher to focus on the turbulence-chemistry interactions in a simplified format. Moreover, it is a simple configuration from the point of view of a modelling approach for computational researchers. Therefore, this jet-in-coflow configuration has been used in many studies with the objective of unraveling the complex mechanisms that stabilize lifted flames produced by a turbulent fuel jet issuing into ambient air.

1.2 Stabilization of Conventional Lifted Flames

The multitude of research endeavors in this area has led to the proposition of several theories regarding the stabilization mechanism of lifted turbulent flames. These theories attempt to provide a clear picture of the governing processes of flame stabilization and destabilization. They have been reviewed in detail by Pitts [2], Lyons [3] and Lawn [4]. In the case of lifted flames, the fuel and air undergo some mixing upstream of the flame base, due to molecular diffusion and turbulent transport. The degree of this fuel/air mixing prior to combustion at the flame base formed the basis some stabilization theories discussed subsequently.

The earliest theory was the premixed flame propagation theory, which was first suggested by Wohl et al. [5] and further promoted by Vanquickenborne and Van Tiggelen [6]. It was suggested that the flame base:

- is completely premixed (Figure 2) and stabilizes in a turbulent region where the composition of the fuel/air mixture is stoichiometric

- propagates upstream with a turbulent burning velocity, which is a function of the laminar flame speed (S_L)
- is stabilized at the point where the turbulent burning velocity is balanced by the incoming gas velocity

Later, Kalghatgi [7] supported this theory and established a relation between the burning velocity and the local Reynolds number and obtained data sets of liftoff heights for different fuels. Observations from several studies have been consistent with the idea of flame propagation playing a role in stabilizing the lifted flame [8] [9] [10] [11]. However, as

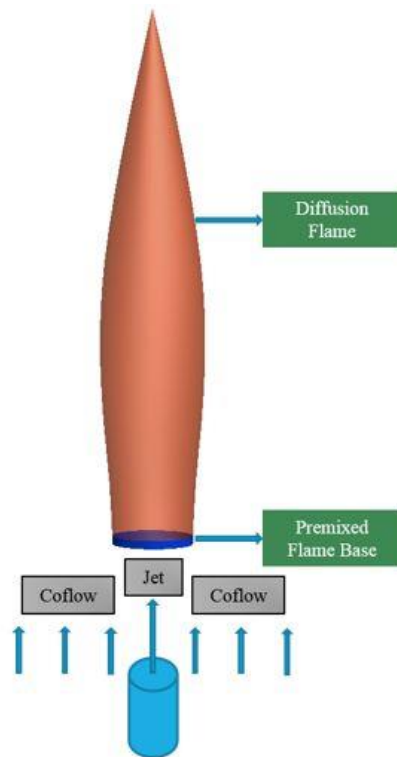


Figure 2: Schematic diagram of the premixed flame base and trailing diffusion flame based on the description given by Vanquickenborne and Van Tiggelen. [6]

pointed out by Hasselbrink Jr. & Mungal [8], this theory does not explain liftoff and blowout that occurs with a sufficient increase of coflow velocity.

The diffusion flamelet theory [13] [14] treats the turbulent flame front as an ensemble of laminar flamelets and suggests that the flame stabilization point is established in the region where the local scalar dissipation rate is sufficiently low such that quenching of the flamelets does not occur. This is also known as the critical scalar dissipation rate theory [14] [15].

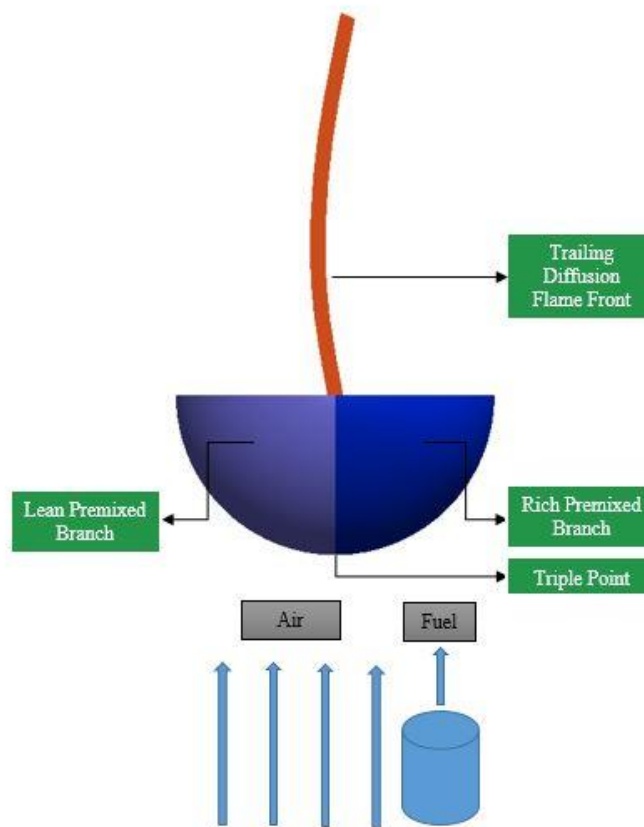


Figure 3: Illustration of the structure of a triple flame based on the illustration of Muñiz and Mungal [12]

Later studies investigated the flame structure around the stabilization point, which led to another alternate theory of flame stabilization (called edge flame propagation theory), which states that a partially premixed leading edge stabilizes the flame [16] [17]. It was observed that the flame structure around its base (stabilization point) had a tribrachial structure which is commonly called ‘triple flame’ [18]. This triple flame has a fuel stratified structure which contains a rich premixed branch (on the fuel side), a lean premixed branch (on the oxidizer side) and a trailing diffusion flame, as shown in Figure 3. Buckmaster [19] reviewed the mathematics of the edge flame structure, stating that the edge propagation speed could be either positive or negative. This is consistent with the observation of Watson et al. [20], who saw advancing and retreating motions of the leading edge of a lifted CH_4 flame through simultaneous Rayleigh imaging and $CH - PLIF$. Watson et al. [21] experimentally observed the tribrachial edge structure in a lifted CH_4 jet flame. Ruetsch et al. [18] used DNS data of a laminar mixing layer to describe the effects of heat release on the propagation of edge flames. They found that heat release in the flammable mixture upstream of the leading edge modifies the flowfield velocity, allowing the edge to propagate faster. Meanwhile, heat release also serves to decrease mixture fraction gradient, which slows down the edge propagation speed, thus stabilizing the flame.

Further studies focused on the physical understanding of turbulent mixing. Miake-Lye and Hammer [22] performed an experimental study on lifted premixed jet flames using methane, ethylene and natural gas and suggested that the stabilization of turbulent lifted jet flames was effected by the passage of large scale structures produced by turbulence. Oscillations in the

flame liftoff height seemed to concur with the idea of the flame base propagating from a large scale structure to another structure upstream of it and being transported downstream. Figure 4 demonstrates the process of partially premixed flame base propagation followed by extinction caused by vortices which precedes further mixing of fuel and air upstream of the new shifted flame base, as illustrated by Kelman et al. [23]. The passage of vortical structures has been observed to cause pinching of the diffusion flame downstream of the stabilization point, leading to local quenching [24]. This theory can thus be linked with the diffusion flamelet quenching theory. Although there is no consensus that the influence of large scale structures is a causative stabilization mechanism, their influence on the flame base has been observed.

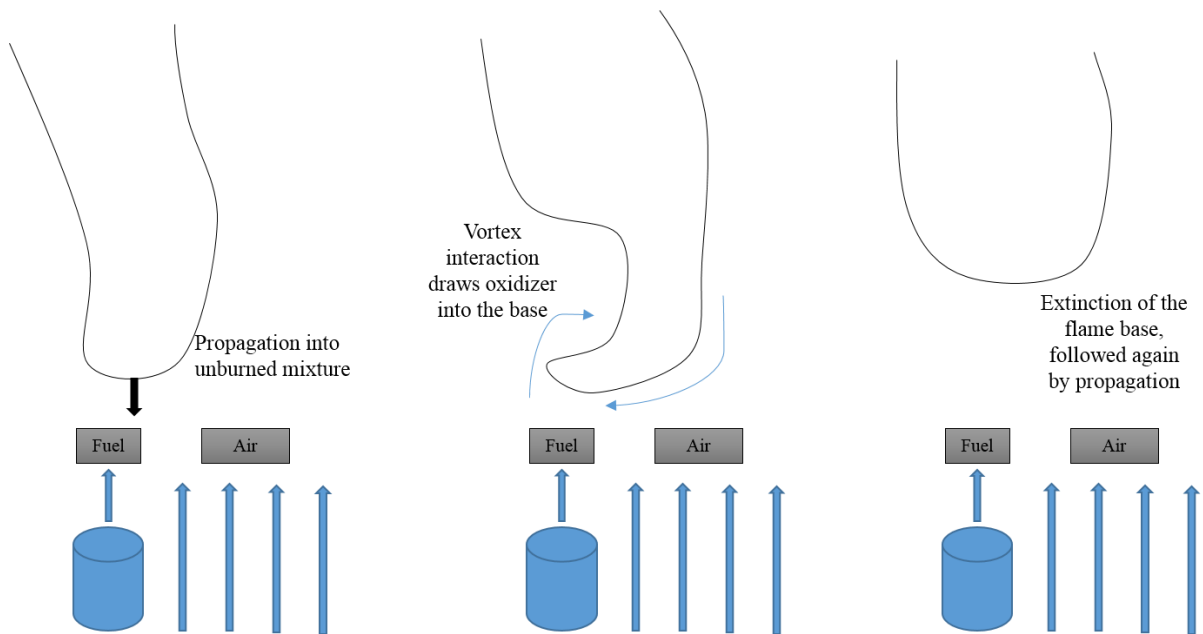


Figure 4: Illustration of a large scale structure influencing the base of a lifted flame based on the illustration by Kelman et al. [23]

1.3 Stabilization of Lifted Jet Flames in High Temperature Environment

Our study focuses on turbulent non-premixed combustion in a vitiated coflow, which have large similarities with classical turbulent lifted flames as well as stark differences in the stabilization mechanisms due to the coflow vitiation (from its high temperature). Therefore, having discussed lifted turbulent jet flames in a coflow of air at ambient temperature (conventional/classical lifted turbulent jet flames), we now look at lifted flames in a high temperature environment.

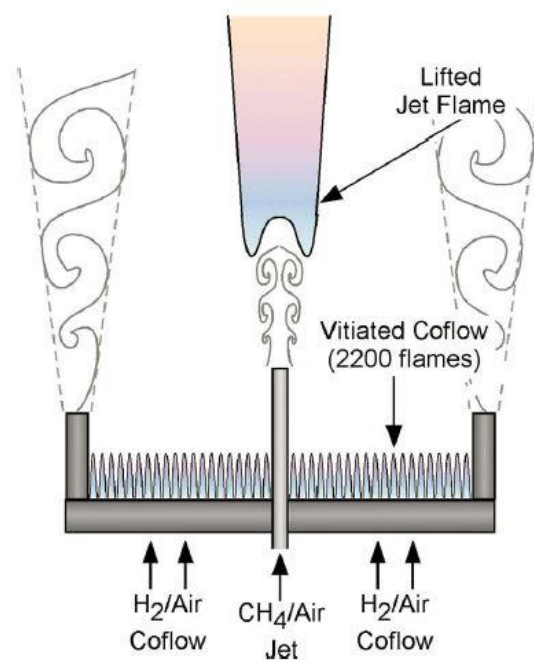


Figure 5: Schematic diagram of a burner with a lifted CH_4 jet flame in a vitiated coflow produced by H_2 /Air combustion. [25]

A striking difference between these two cases was pointed out by Oldenhof et al. [26] who performed an experimental study with a jet of Dutch natural gas and showed a temporal

evolution of the jet flame liftoff height in a vitiated coflow and compared it against the corresponding liftoff height evolution for a conventional lifted jet flame. This comparison, shown in Figure 6, shows a sawtooth profile for the case of the hot coflow. By contrast, the liftoff height is extremely stable in cold coflow. This illustrates the unsteadiness of the lifted flame base in high temperature coflow and the existence of complex flame stabilization mechanism active in this configuration.

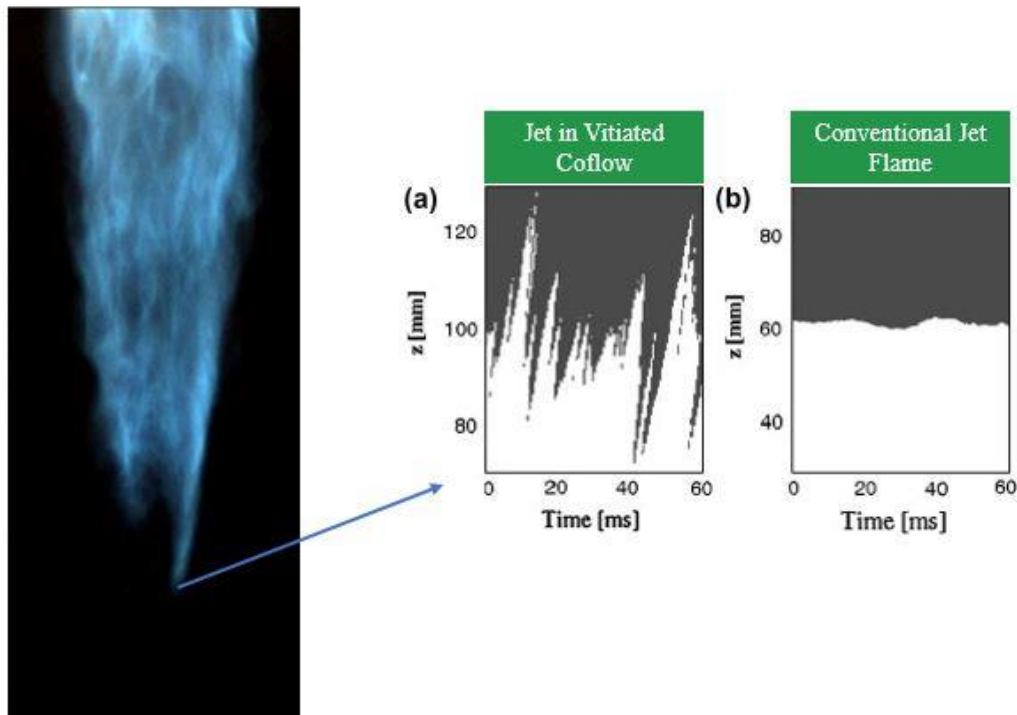


Figure 6: Comparison of temporal evolution of liftoff height of a jet flame in vitiated coflow (left) vs cold coflow (right). [26]

Some of the recent efforts focused on understanding the flame stabilization/destabilization in a heated coflow at moderate ($T_{oxidizer} < 1000\text{K}$) and high temperatures ($T_{oxidizer} \geq 1350\text{K}$) that are much larger than the fuel crossover temperature. Lamige et al. [27] performed OH-PLIF and high-speed CH^* -chemiluminescence imaging of a CH_4 jet flame with coflow (air)

temperature up to 1000 K. They reported that the flame liftoff height decreased with increasing coflow temperature, consistent with faster kinetics at higher temperatures. They further reported a significantly different destabilization of the flame through splitting that resulted in flame liftoff. It should be noted that despite the coflow temperature being considerably larger than autoignition temperature of methane, the authors did not observe the autoignition phenomenon during their experiments. The stabilization/destabilization of the flame base occurred dominantly due to partial premixing.

The role of autoignition in the stabilization of turbulent flames was suggested by Masri et al. [29] and Cabra et al. [25] [30]. There has since been extensive research done to understand the autoignition phenomenon. The role of autoignition in the initiation of turbulent non-premixed combustion has been extensively reviewed by Mastorakos [31]. Several studies

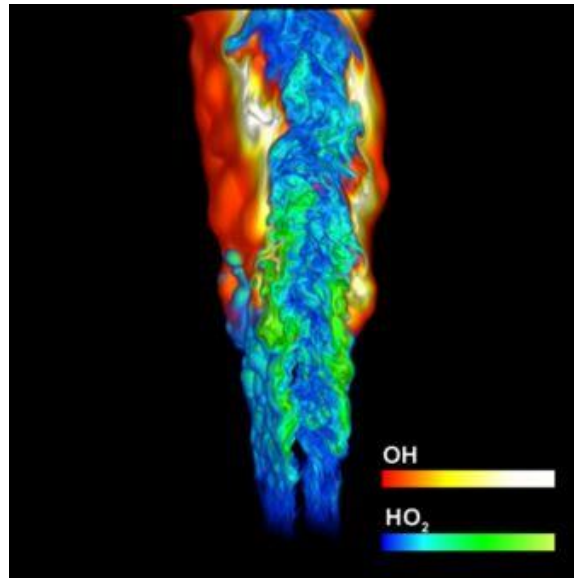


Figure 7: DNS mass fraction plot showing HO_2 radical buildup upstream of the flame base of an ethylene jet in a heated coflow. [28]

reported over the last decade have suggested that autoignition is the dominant flame stabilization mechanism for lifted flames in heated/vitiated coflow. Nearly all studies so far on reported autoignition-based flame stabilization have been made at oxidizer temperature significantly exceeding the crossover temperature of the jet fuel. Yoo et al. [32] studied how the different radicals within the autoignition kernel interact with the flame base of a lifted H_2 jet flame using DNS. They showed that the heat release near the mean flame base is caused by autoignition; further downstream of the flame base, partial premixing and non-premixed combustion cause most of heat release with non-trivial contribution from autoignition. Yet another DNS study performed by Yoo et al. [28] on an ethylene jet flame in a highly heated coflow ($T_{oxidizer} = 1550$ K) demonstrates the formation of a radical pool of perhydroxyl (HO_2) far upstream of the observed flame base, indicating a strong role played by autoignition in flame stabilization since HO_2 is an important intermediate species in the autoignition of ethylene-air mixtures. Additionally, as seen in Figure 7, pockets of high OH mass fraction can be observed upstream of the well-defined high OH region. This indicates the formation of autoignition kernels. Experimental visualization studies of Oldenhof [26] on Dutch natural gas jet flames further showed the stabilizing flame base response with the passage of autoignition kernels. Computational studies by Gordon et al. investigated convection-diffusion-reaction (CDR) budgets and they inferred that there was a significant effect of autoignition in stabilizing turbulent jet flames across a range of coflow temperatures (1030 K, 1045 K and 1080 K) in H_2 jet flames [33] and at 1355 K in CH_4 flames [34]. Domingo et al. [35] performed a large eddy simulation (LES) of a CH_4 jet in vitiated coflow and suggested that autoignition may begin the combustion, after which stabilization could be

dominated by either autoignition or partially premixed flame propagation. They also stated that it was possible for propagation to take over when autoignition could not occur. Conditional moment closure (CMC) simulations of a H_2/N_2 jet flame in vitiated coflow by Patwardhan et al. [36] suggested that the stabilization of turbulent jet flames in hot coflow was mainly dominated by turbulent premixed flame propagation at low temperatures (1025K) and by autoignition at higher temperatures (1080 K). Thus, there appears to be overall consensus on autoignition being the primary flame stabilization mechanism at coflow temperatures far exceeding the crossover temperature.

There is very little effort on the flame stabilization mechanisms at oxidizer temperatures close to the crossover temperature that is in between exclusively partially premixed and autoignition stabilized ($T = 1000 \text{ K} - 1350 \text{ K}$) This situation has common occurrence close to the walls of conventional and low temperature combustors and at phases away from top dead center of conventional diesel engines; understanding the combustion at this temperature realm is also critical towards widening the operating temperatures of the low temperature clean combustors to smaller temperatures. In this temperature range, we expect to have interesting interplay between partial premixing and autoignition and other potential stabilization mechanisms. This flame regime is referred to as “autoignition-assisted flames” in this manuscript. The objective of this work is to address the issue of flame stabilization mechanisms in autoignition-assisted flames. The questions that this thesis seeks to answer include:

- 1) What are the global features of flame base motions in an autoignition-assisted flame regime? Are there certain characteristic motions that are different from exclusively partially premixed and dominantly autoignition-stabilized flames?

- 2) What mechanisms contribute to the stabilization of the flame base and how do the different mechanisms interact with one another?

- 3) How do global parameters such as coflow temperature, jet Reynolds number, and O_2 mole fraction favor or inhibit different stabilization mechanisms?

2 EXPERIMENTAL METHODS

2.1 Experimental Setup

An experimental setup was designed and fabricated for the purpose of this study. This setup is called the Jet In Vitiated CoFlow burner (JIVCF). JIVCF was made to model the vitiated coflow burner used by Cabra et al. [25] and documents containing details of their burner design [37] [38] were consulted during the design and fabrication of our experimental setup. However, there are considerable differences in the designs of the Cabra burner and our JIVCF. A schematic of the experimental setup is shown in Figure 8.

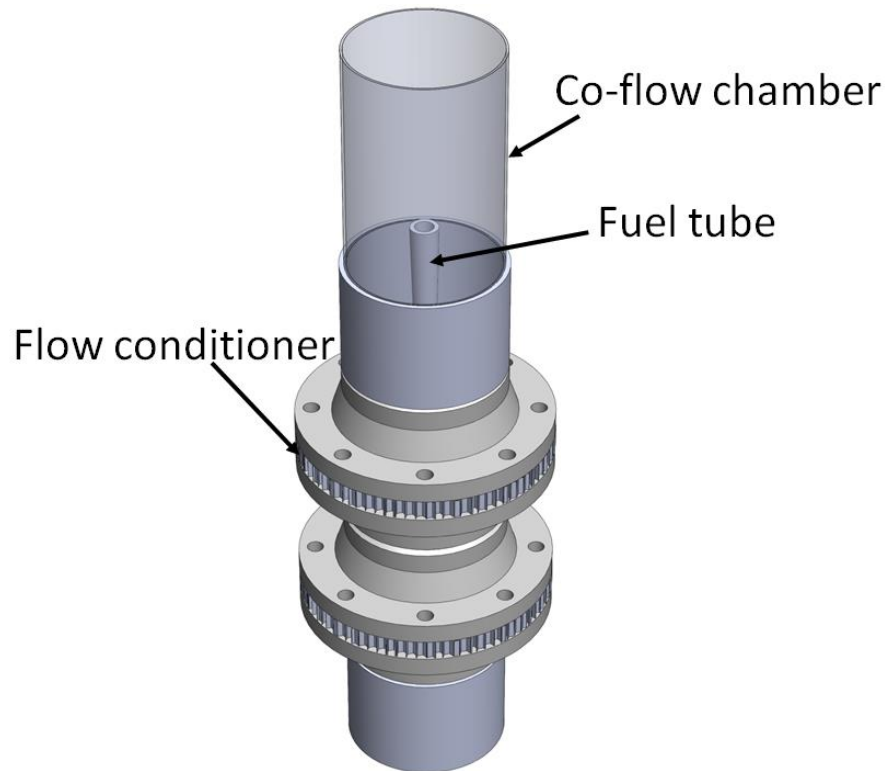


Figure 8: Schematic of the Experimental Setup

The vitiated coflow was produced by lean premixed combustion of a CH_4/Air mixture. This premixed flame was stabilized $\sim 165\text{ mm}$ upstream of the jet exit. Thus, in comparison to the conventional and heated jet-in-coflow configurations, the JIVCF creates a coflow containing significantly lower percentages of oxygen by volume, i.e. lower O_2 mole fractions and significantly high temperature. These low X_{O_2} and high temperature conditions are highly relevant for investigating combustion phenomena that occur in gas turbine afterburners, clean combustors and diesel engines that employ exhaust gas recirculation and are therefore apt for our purposes.

Since the coflow is produced by a premixed flame, we must address one of the major concerns in premixed combustion, namely flame flashback. Premixed flames propagate towards the incoming reactants since the tendency of the flame is to sustain itself by consuming reactants. This phenomenon is potentially dangerous because:

- Flashback causes a pressure and temperature rise in the burner which can cause structural damage.
- If the flame comes into contact with a sufficiently large volume of the reactant mixture, a minor explosion can occur.

Therefore, undertaking measures to prevent flashback is of utmost importance. The JIVCF burner was thus designed to eliminate the risk of flashback.

The design of the JIVCF took the following major points into consideration:

1. A uniform and well mixed reactant flow must be provided for the coflow flame.

2. The setup must sustain a lean premixed coflow flame.
3. The fuel jet must issue into an environment of uniform thermochemical conditions.
4. Entrainment of ambient air must be avoided, especially until the jet exit plane.
5. The setup must have a wide range of operating conditions.
6. The jet flame must be optically accessible.
7. Safety must be ensured.

A brief description of the various parts of the experimental setup follows, with illustrations and the considerations behind the aspects of their design.

2.1.1 Perforated Copper Plate (Flame Holder)

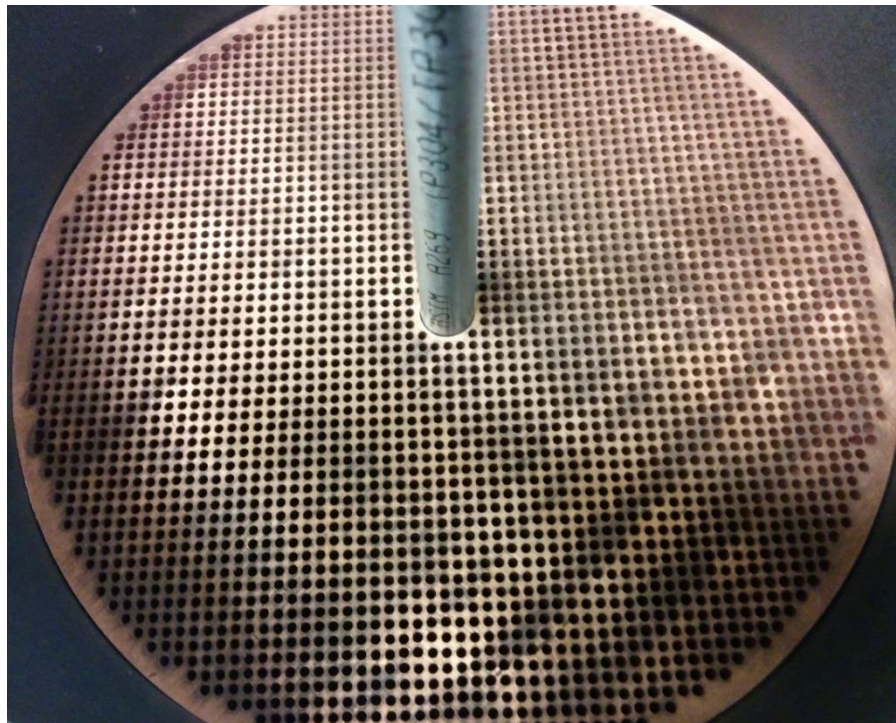


Figure 9: Copper Flame Holder Plate

The coflow flame was stabilized on a perforated copper plate. The plate, 6" (152.4 mm) in diameter and 3/8" (9.525 mm) thick, contains ~3500 holes of 1 mm diameter with a resulting blockage of 75%. This flame holder was manufactured using water jet machining. The size of each hole was selected to be 1 mm in order for it to be safely below the quenching diameter for premixed CH_4/Air flames, which is 2 mm [39]. The coflow flame was not in contact with the surface of the flame holder, but is lifted very slightly (of the order of 1mm) off the surface. The very small diameter of the holes in the plate gives the advantage of being able to accommodate a large number of holes on the plate. As a result, all the holes put together have a very large surface area. This, along with the high thermal conductivity of copper ($401 W/mK$), aids in rapidly dissipating heat and quenching the flame in the event of flashback.

The following theoretical considerations were made for designing the perforated plate. A premixed flame propagates at a velocity whose magnitude is called the laminar flame speed (S_L) and whose direction is upstream, i.e., towards the reactant stream. Therefore, in order to avoid risk of the flame flashing back into the mixing chamber, the velocity of the reactant mixture is always set to be sufficiently higher than S_L for any given coflow case. The laminar flame speeds for each equivalence ratio of the CH_4/Air mixture were obtained from Vagelopoulos and Egolfopoulos [40]. This measure greatly minimizes the chances of flashback.

Designing the flame holder plate to have a blockage of 75% assisted the stabilization of the coflow flame in the following two ways:

- The coflow mixture accelerates through the holes in the plate. From continuity, it can be shown that the velocity increases as follows:

$$\frac{u_{hole}}{u_{bulk}} = \frac{1}{1 - blockage} = \frac{1}{1 - 0.75} = 4$$

So the bulk velocity of the coflow reactant mixture increases by a factor of 4 through the copper plate. This ensures that the coflow flame is not susceptible to flashback since the ratio of mixture velocity to the laminar flame speed becomes sufficiently high.

- The space between the holes provides space for recirculation of high temperature products from each of the flames that constitute the bulk coflow flame, as shown by Cabra [38]. This recirculation assists in stabilizing each flame, thereby stabilizing the entire coflow flame on the plate.

2.1.2 Ceramic Honeycomb Flow Conditioner

In order to obtain a flat and uniform coflow flame, the reactant mixture must be conditioned to remove turbulence. For this purpose, two ceramic flow conditioning honeycombs were installed upstream of the copper plate. Each of these honeycomb blocks is

2" (50.8 mm) thick, and contains square channels that run straight along their lengths at a cell density of 230 CPSI (cells per square inch). They were purchased from Applied Ceramics Inc. as square pieces of 5.91" x 5.91" dimension. Using waterjet machining, the largest possible circle was cut out of each honeycomb and a hole was drilled in their centers to allow the center fuel tube to pass through. The honeycombs are placed on an aluminum ring to hold them in place inside the burner.



Figure 10: Ceramic Flow Conditioner

2.1.3 Flow Control System

The air supply for the coflow mixture is taken from the compressed air outlet in the laboratory. Compressed air at 80 psi is regulated down to 20 psi and then flows through a

needle valve, air filter, mass flow meter and a check valve. The CH_4 gas from the cylinder is split into two streams - one for the coflow and the other for the center jet. Both these streams flow through a needle valve, mass flow meter and a check valve. [NOTE: The mass flow meters were calibrated for N_2 , hence a multiplication factor of 0.72, as given in the instruction manual, had to be used to set flow rates for methane. For air, the multiplication factor was 1.] Downstream of the check valves, the methane stream for the coflow joins the air stream and the mixture is transported to the mixing chamber of the burner. During experiments in which the coflow was diluted with N_2 , a separate gas line for N_2 joins the CH_4/Air mixture before entering the burner.

The mass flow meter ranges are as follows:

- Air - 0-1000 SLPM
- CH_4 (coflow) - 0-50 SLPM
- CH_4 (jet) - 0-100 SLPM
- N_2 - 0-50 SLPM

(SLPM = standard liters per minute)

These ranges are sufficient for experiments to be performed over a wide range of jet velocities, and coflow equivalence ratios, compositions and velocities.

2.1.4 Mixing Chamber

The mixing chamber was initially designed to be an 18" long pipe section, 6" in inner diameter. This length was chosen in order to provide sufficient time for the air-fuel mixture to mix thoroughly. The chamber was later modified to comprise of three pipe sections, each 6" in length and 6" in inner diameter. This was done in order to accommodate two sets of pipe flanges. These flanges hold steel wire meshes which function as a turbulence grid. Inducing turbulence in the flow enhances mixing of the reactants prior to reaching the copper plate.



Figure 11: Mixing chamber with the air-fuel mixture entering it tangentially.

The air-fuel mixture enters the bottom section of the mixing chamber through a 1/2" outer diameter tube. This tube was welded to the mixing chamber at such an angle that the flow enters tangentially into the chamber. This provides a longer residence time for the flow inside the chamber, enhancing the mixing process.

2.1.5 Fuel Jet

The fuel selected for the jet in the JIVCF was methane (CH_4). The fuel flows through a 3/8" outer diameter stainless steel tube. The tube has an inner diameter of 0.209" (5.3 mm) and its inner surface is seamless, thus ensuring that the flow through the tube maintains a uniform profile. This fuel tube runs through the entire length of the burner, at the center of its

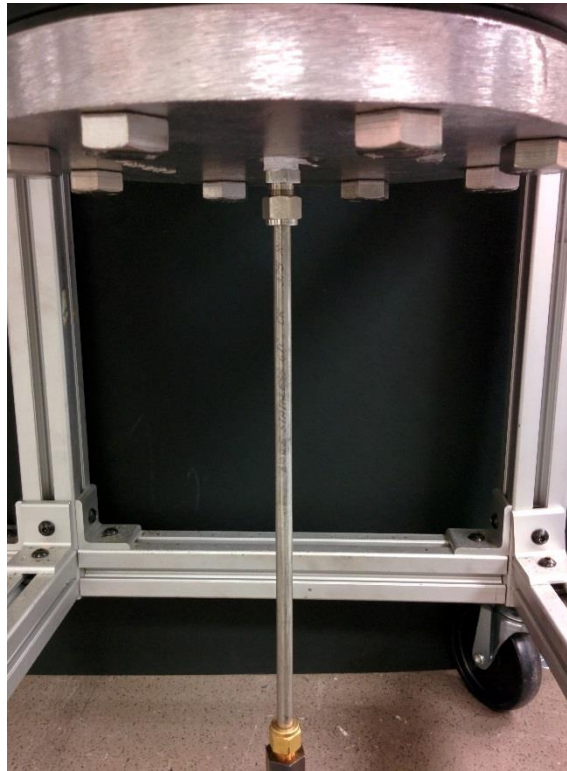


Figure 12: Fuel jet tube entering the burner through the bore-through connector

cross section. The mixing chamber is closed at the bottom by a cap flange. At the center of the cap flange, a bored through connector for 3/8" OD tube is installed. The fuel tube passes through and is held in place by this connector. The height of the fuel tube can be adjusted easily by loosening the nut on the bored through connector, moving the tube to the desired height, and then tightening the nut.

Tests performed by Cabra [38] suggested that 45 diameters could be a sufficient length for the coflow product stream to attain equilibrium. Thus, the jet exit was placed at a height of 6.5" (~165mm) above the flame holder plate, giving it more than three times the suggested length. This should ensure that the fuel jet issues into a uniform environment, and temperature measurements performed at the jet exit plane support this conjecture.

2.1.6 Exit Collar

In order to shield the coflow flame and the product stream from entrainment of ambient air, an exit collar made of steel is placed on the copper plate. The collar sits on the plate by a lip and sink connection, employing a step machined into the outer rim of the copper plate. The collar extends up to a height of 6" above the plate and shields the coflow almost up to the jet exit plane. Since our experiments focus on the base of the lifted jet flames, opacity at and beyond the jet exit plane would be highly inconvenient for imaging purposes. This was the limiting factor in determining the height of the exit collar. However, soon after the work reported in this document was completed, this steel exit collar was replaced by an optically accessible fused quartz tube mounted on a steel adapter plate.

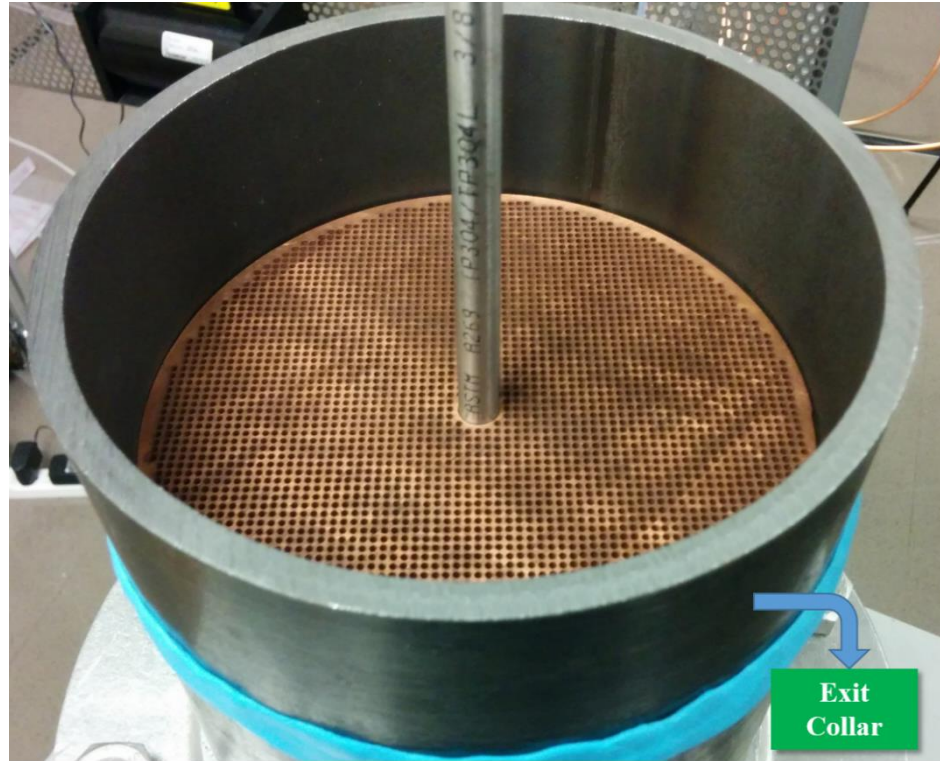


Figure 13: Steel Exit Collar

2.1.7 Summary

To summarize the key points regarding the experimental setup, the vitiated coflow was produced by lean premixed combustion of a CH_4/Air mixture on a perforated copper plate. A stainless steel tube (9.525 mm O.D. and 5.309 mm I.D.) passes through the center of the perforated plate. A turbulent jet of CH_4 issues out of this tube 165 mm above the copper plate. A steel exit collar placed on the plate shields the coflow flame from ambient air entrainment. The CH_4 jet auto ignites in the high temperature environment, producing a turbulent lifted jet flame.

2.2 Coflow Exit Conditions

In order to perform investigations of the turbulent jet in a high temperature environment of combustion products, it is essential to first establish the characteristics of the flow field surrounding the jet fuel upon its exit from the center tube. Moreover, characterization of the initial and boundary conditions of the flow field is required in order to facilitate numerical modelling studies using this burner configuration. Hence, prior to carrying out the experiments reported in this document, the temperature profile of the vitiated coflow was measured.

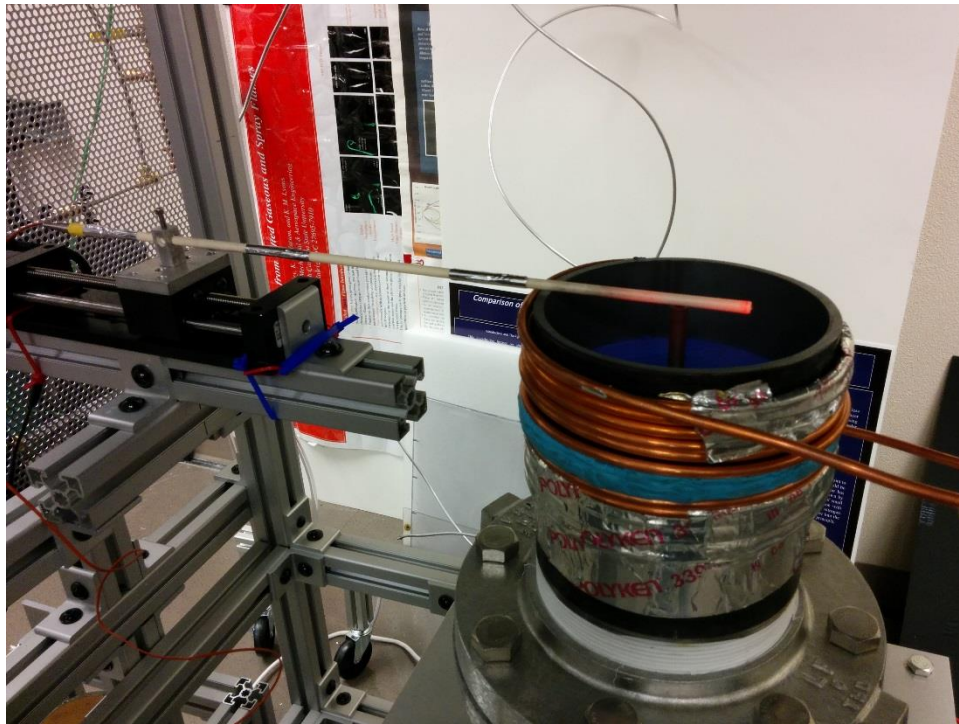


Figure 14: Thermocouple measurements

Temperature measurements were performed for the case where the coflow fuel mixture was set at an equivalence ratio of $\phi = 0.5$, resulting in an adiabatic flame temperature of 1475 K. The temperature of the hot gaseous mixture of combustion products from this flame was measured using a K-Type thermocouple at an axial distance of 5 mm ($\frac{x}{D} \approx 1$) from the jet exit plane. The measurements were obtained at an interval of 0.5" (12.7 mm) along the radial direction. This provided sufficient spatial resolution to characterize the flow field.

The position of the thermocouple bead was moved using a translation stage which was controlled using the IMS Terminal software. Although it is ideal to have the thermocouple wire (with its insulation) pointing downwards from a height and translating this horizontally along the radial profile of the burner, this could not be done due to practical difficulties. So, an alternative method was employed in which the length of the thermocouple wire was moved across the face of the burner, as shown in Figure 14. This could cause some inaccuracies, especially after the thermocouple bead has crossed the center jet. This is due to the fact that while a large portion of the thermocouple is in a highly heated environment, a portion in between is in contact with a relatively much cooler jet, and conduction through the thermocouple could lead to inaccurate measurements. In order to combat this issue, the thermocouple wire was encased in a ceramic insulation sleeve, with only small length near the tip being exposed.

At several points of measurement, the thermocouple bead was found to be radiating. This radiation was accounted for and the appropriate correction was performed using the

procedure described by Jha et al. [41]. Figure 15 shows the measured temperature profile after radiation correction. It can be seen from Figure 15 that the measured temperature is about 300 K lesser than the adiabatic flame temperature. We believe this depreciation is because of the residual radiation losses that remained after radiation correction. The radial temperature profile was found to be reasonably flat up to a radial position of 2" (~50 mm) from the jet centerline. This indicates that the fuel jet issues into a thermally uniform environment of combustion products.

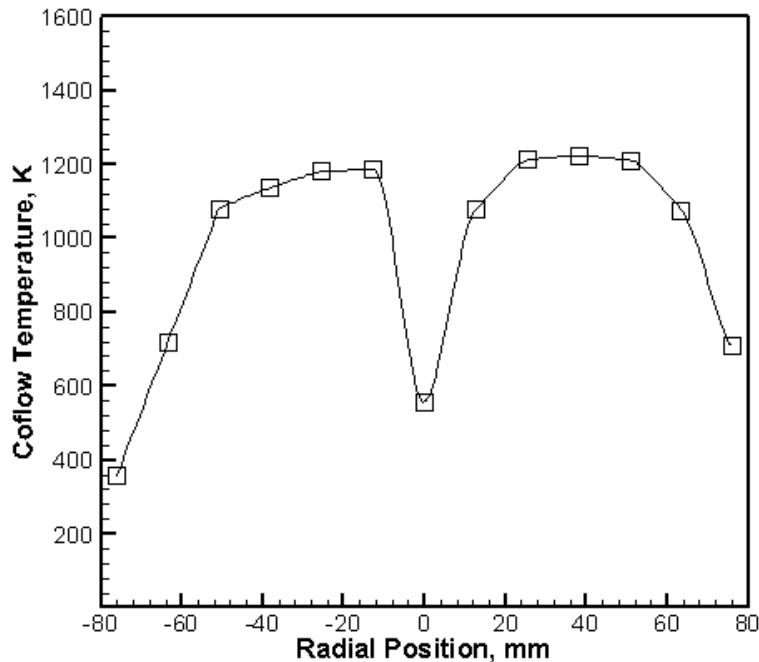


Figure 15: Radial temperature profile of the vitiated coflow. These measurements were taken for a coflow equivalence ratio of 0.5. The coflow adiabatic flame temperature for this case was 1475 K.

The effect of ambient air entrainment into the coflow can be seen near the boundary of the coflow, where there is a significant decrease in the measured temperature. Despite using an

exit collar, some amount of entrainment of ambient air appears to be unavoidable. However, its effect on the flow field is sufficiently removed from the fuel jet and this decrease in temperature at the boundaries can be assumed to have no effect on the combustion process of the jet.

After obtaining the temperature profile of the coflow, numerous experimental investigations of the turbulent jet flame in vitiated coflow were performed.

[NOTE: The velocity field of the coflow has not been characterized yet for the JIVCF. At this point, a particle image velocimetry (PIV) setup is in the process of being assembled for local velocity field measurements of the lifted jet flame base, and the coflow velocity field characterization will also be performed along with these studies.]

2.3 Tests Performed

A set of experiments was conducted across a matrix of test conditions. The test matrix was obtained by varying two parameters:

- Coflow Equivalence Ratio (ϕ)
- Jet Reynolds Number (Re_D)

It must be noted that changing the equivalence ratio of the CH_4/Air coflow reactant mixture in turn results in a change in the following two quantities which are of interest to us:

- Coflow Adiabatic Flame Temperature (T_{co})
- Coflow Oxygen Mole Fraction (X_{O_2})

For the test cases reported here, the equivalence ratio (ϕ) ranged from 0.5 to 0.625, resulting in a T_{co} range of 1475 K to 1705 K and an X_{O_2} range of 7.39% to 9.98% (X_{O_2} decreases with increase in ϕ). For each test campaign, the CH_4 jet was issued at two Reynolds numbers – $Re_D = 4500$ and 8000. Table 1 lists the flame configurations that were tested for this study.

Table 1: Test Matrix

Flame Number	Coflow Equivalence Ratio (ϕ)	Coflow Adiabatic Flame Temperature (T_{co})	O_2 Mole Fraction (X_{O_2})	Jet Reynolds Number (Re_D)
1	0.500	1475 K	9.98%	4500
2	0.500	1475 K	9.98%	8000
3	0.575	1615 K	8.42 %	4500
4	0.575	1615 K	8.42 %	8000
5	0.625	1705 K	7.39%	4500
6	0.625	1705 K	7.39%	8000

For each of the above test cases, several images of the jet flame were acquired and studies were performed based on flame luminosity.

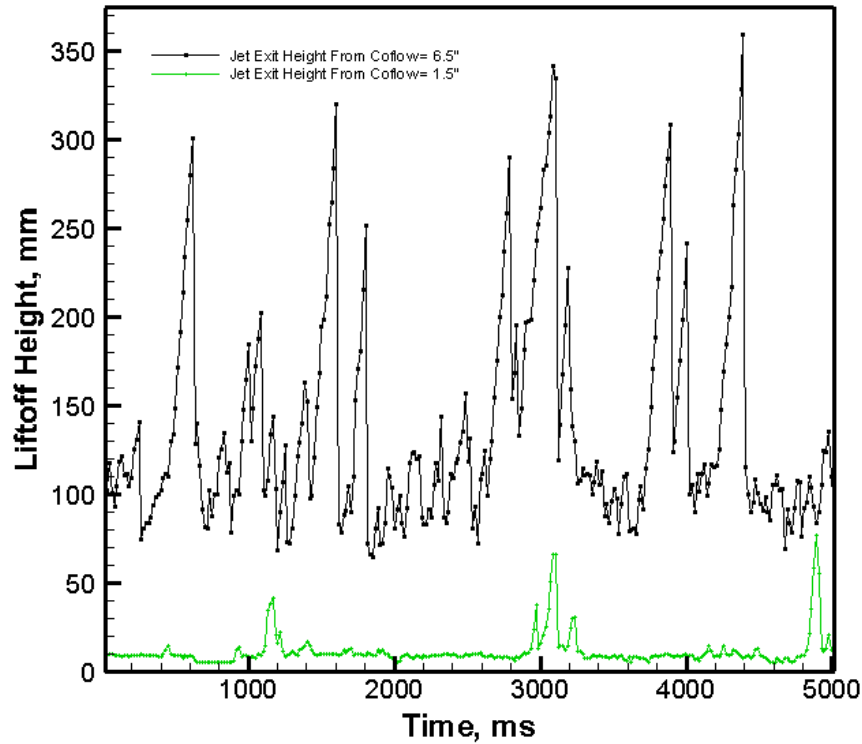


Figure 16: Temporal evolution of flame liftoff height for two cases: 1) $\phi = 0.625$, $T_{co} = 1705$ K, jet exit height from coflow = 6.5" (165 mm) and 2) $\phi = 0.5$, $T_{co} = 1475$ K, jet exit height from coflow = 1.5" (38 mm)

In order to justify the values of coflow adiabatic flame temperature used in our experiments (Table 1), we can compare the two plots of liftoff height evolution with time shown in Figure 16. The details of how the liftoff height was obtained will be discussed in subsequent sections. At this point, this comparison serves to illustrate the clear difference in combustion regime obtained by changing the height of the fuel jet exit with respect to the coflow flame. At 1.5" above the coflow flame, the jet flame is only lifted by about $\frac{x}{D} \sim 2$ (where D is the jet diameter), with very low fluctuations about a mean liftoff height. On the other hand, we see drastic changes in the flame liftoff height with time when the jet exit is moved to 6.5"

downstream of the coflow flame. The temperature of the coflow at a height of 1.5" above the coflow flame will be closer to the adiabatic flame temperature than at a height of 6.5", due to lower heat loss. Even though the adiabatic flame temperatures for the two cases plotted in Figure 16 are not the same, it must be noted that for the first case (1.5"), the adiabatic flame temperature is the lowest of the values in Table 1 ($T_{co} = 1475 K$) and for the second case (6.5"), it is the highest ($T_{co} = 1705 K$). Additionally, the trend of liftoff height evolution observed at jet exit height of 6.5" was consistent for all the test cases listed in Table 1, which gives us a compelling reason to believe that despite the high values of adiabatic flame temperature, our experimental cases lie in the regime that we are interested in studying.

2.4 Image Acquisition and Processing

Raw images of the jet flame were recorded using a CCD camera (JAI Inc., Model: CB-040GE), at a recording rate of 60 Hz. The record length was set at 25 seconds, therefore 1500 images were acquired for each test condition. The field of view of the camera was set based on the objective of being able to observe sufficient downstream length of the jet flame as well as being able to capture small autoignition kernels, considering the resolution of the camera. It is essential to obtain instantaneous images in order to be able to successfully identify small changes in the flame structure and to visually observe the formation of autoignition kernels. This becomes difficult at high exposure times since the degree of

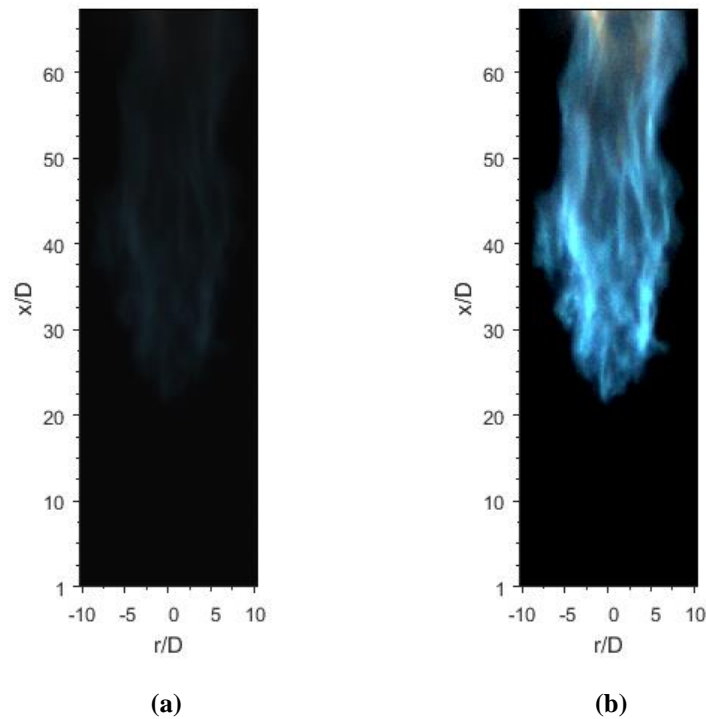


Figure 17: Comparison of raw image obtained from camera and the contrast stretched image after processing using ImageJ

instantaneity of the images decreases. However, since a low exposure time setting was seen to result in very dim images, a balance was struck at 10 ms exposure time so as to obtain sufficiently bright and instantaneous images. All the jet flame images shown in the Results & Discussion chapter of this document were obtained by taking the raw images from the CCD camera and contrast stretching it for better viewing. This was done using the ImageJ software [42]. A comparison of a raw image and its contrast stretched image counterpart shown in Figure 17. It must be noted here that the contrast/brightness stretching used on the images were identical; therefore, the brightness of the image directly correlates with flame luminosity.

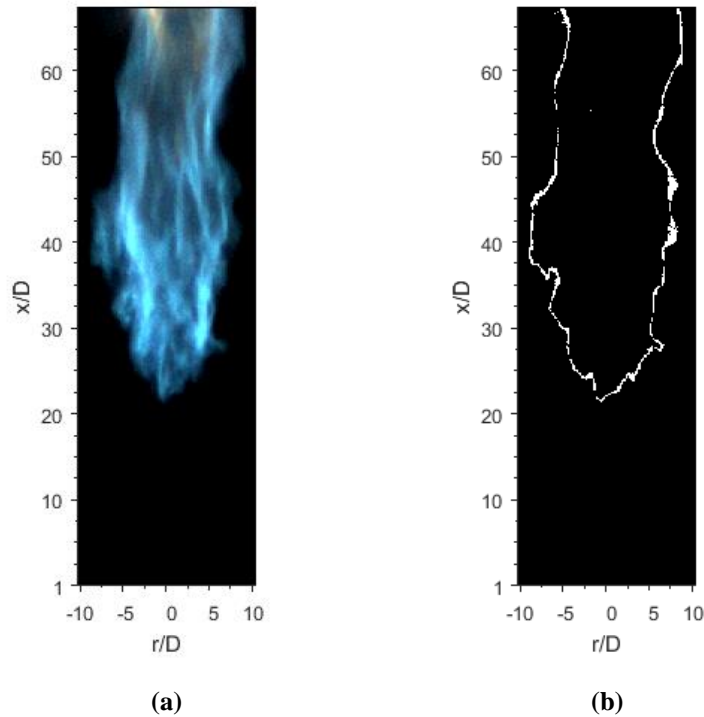


Figure 18: Flame luminosity image and the corresponding binary image of the flame edge

These images were converted to greyscale, and the background image was then subtracted from each of the flame images using in-house codes. Using Matlab's *edge* function, a Sobel filter was employed to detect the high spatial gradient regions in the flame images and convert them into binary images, which were then processed to study the global features of the flames. A sensitivity threshold was applied to the output of the Sobel filter. The purpose of this thresholding was to eliminate edges that had gradients smaller than the threshold, thereby outputting a binary image containing only sharp gradients, allowing us to detect the flame edges with good accuracy and discard noise. The filter sensitivity threshold value was iteratively determined and we converged at a value of 0.02. The selection of this threshold value was also dependent on its effectiveness in locating the edges of autoignition kernels. Figure 18 shows the flame luminosity image and its edge detected after data processing. It can be observed visually that our codes do a reliable job in detecting the flame luminosity edges without introducing extraneous features in the edge and being able to overcome the noise-induced artificial edges.

For investigations on the basis of flame liftoff height, the flame base location was determined as the lowest axial distance where the flame edge was observed. In the case of images that contained an autoignition kernel upstream of the main flame, the kernel was discarded and base of the main flame edge was taken to be the flame base location. Using this method of processing the flame luminosity images, we made several global observations regarding the mechanisms involved in the flame stabilization of turbulent jet flames in a vitiated coflow.

3 RESULTS AND DISCUSSION

3.1 Global Observations of the Lifted Jet Flames

Flame luminosity imaging over the test matrix (Table 1) was performed and images of the flame edges were obtained by processing the raw jet flame images using Matlab. The flame edge images were analyzed in order to obtain insights into the global features of lifted jet flame stabilization, by studying the motions of the flame base. The temporal resolution of the image sequence was adequate to delineate the large-scale bulk motions of the flame base. Through flame luminosity imaging, we observed different characteristic bulk flame base motions (referred herein as “modes”). By noting the flame base location for each image in the sequence, we plotted the temporal evolution of the flame liftoff height, as shown in Figure 19. We will use this plot to identify three modes which were observed and then explain them in further detail.

While we observed essentially same characteristic motions of the flame base across most of the test matrix configurations, which correspond to different modes of flame stabilization, the fractional duration that the flame exhibits the different characteristic motions changed between test cases. The following discussions elucidate the three different modes for a representative test condition with fuel jet $Re_D = 4500$ and coflow adiabatic flame temperature $T_{co} = 1705$ K and oxygen mole fraction $X_{O_2} = 7.39$ % (Flame #5, Table 1).

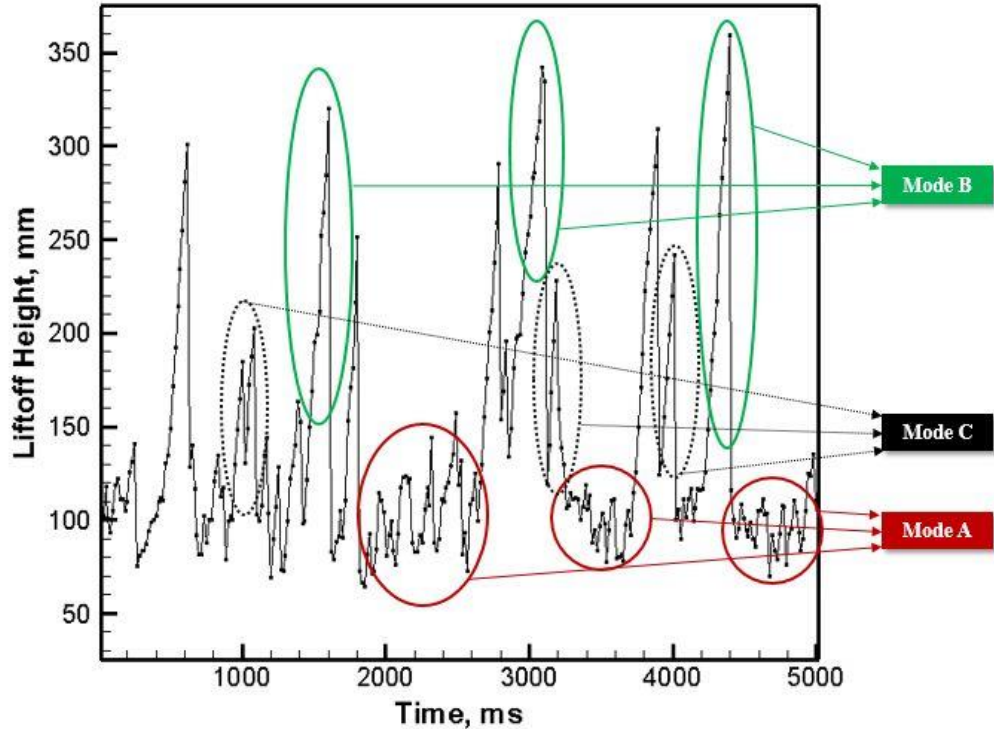


Figure 19: Time series of liftoff height for equivalence ratio of 0.625 at a Reynolds number of 4500. The coflow adiabatic temperature for this case is 1705 K. This time series shows the occurrence of the three flame modes.

3.1.1 Stable Flame Base (Mode A)

Figure 19 highlights some portions of the liftoff height time sequence in which the flame was observed to be executing Mode A motions. This is characterized by very low fluctuations of the flame base about a mean liftoff height. A sequence of images from the representative test case where Mode A can be visually observed is presented in Figure 20. Figure 20 also shows the presence of two stems (marked in image (a) and visible in all other images in the sequence) that extend upstream from the flame bulk, which resembles an edge flame propagating upstream into the fuel stream. The flame base behavior characterized by low fluctuation, and the presence of the two stems on either side of the centerline share

significant similarities with classical turbulent lifted flames studied extensively in the past [19] [3], where the flame is exclusively stabilized by fuel/oxidizer premixing.

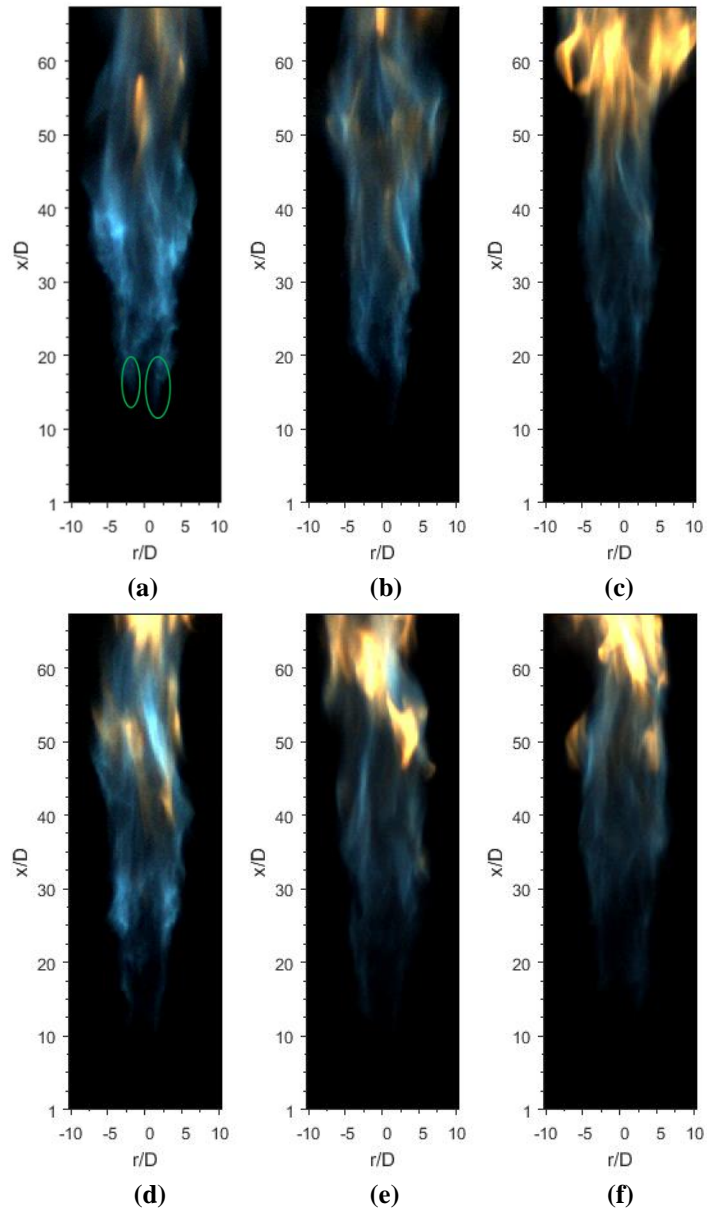


Figure 20: Image sequence demonstrating the lifted turbulent jet flame exhibiting Mode A. Low fluctuations of the flame base can be seen here. Flame stems are marked in image (a).

This observation led us to conjecture that partial premixing induced flame stabilization could be a possible source that induces the characteristic low flame base fluctuations seen in Mode A. However, a numerical study of a H_2/N_2 jet in a vitiated coflow by Gordon et al. [33] documents a similar case in which the jet flame was seen to be quiet and stable. However, they found that even though these characteristics pointed to the possibility of partial premixing of the fuel/oxidizer being the primary mechanism of flame stabilization, the convection-diffusion-reaction (CDR) budgets and radical build-up history clearly pointed toward autoignition as the primary stabilization mechanism. Therefore, we cannot rule out the possibility that the low flame base fluctuations could be a result of the flame being stabilized by the rapid formation of autoignition kernels. This suggestion was also supported by Yoo et al. [32], who also reported similar fluctuation amplitudes in H_2/N_2 flames that are predominantly stabilized by autoignition. We can potentially investigate this mode at a significantly higher imaging rate to visually confirm ignition kernel formation. However, at this point, we cannot make a conclusive statement about the stabilization of Mode A flames from flame luminosity imaging alone. We make a more detailed investigation of the dominant flame stabilization mechanisms during Mode A subsequently, using chemical kinetics to complement the observations from flame luminosity.

3.1.2 Flame Blowout (Mode B)

Often, the nominally stable flame base exhibiting “Mode A” motions gives way to an avalanche downstream motion, which resembles a blowout sequence in classical turbulent lifted flames. While the avalanche downstream motion of classical turbulent flames always

leads to global flame extinction, in our flames we observed two possible outcomes – 1) a global extinction of the flame similar to classical flames (referred to as “Mode B”); and 2) one or more autoignition kernel(s) re-anchors the flame base and arrests the blowout process. In this thesis, the term ‘blowout’ is taken to mean the destabilization and subsequent liftoff of the jet flame to an axial location beyond the field of view of the CCD camera ($x/D > 68.5$). Sections of the flame liftoff height time sequence which represent Mode B motions are marked in Figure 19. It must be noted here that the final image of a blowout sequence is followed by blank images that precede a relight of the flame. These blank images were always discarded in our analysis and evaluation of liftoff height, therefore it appears that the flame base jumps from a high downstream location to a location much closer to the jet exit, while this does not actually happen in Mode B. Figure 21 shows an image sequence of the flame executing Mode B motions and Figure 22 is the sequence of flame edge binary images corresponding to the sequence shown in Figure 21.

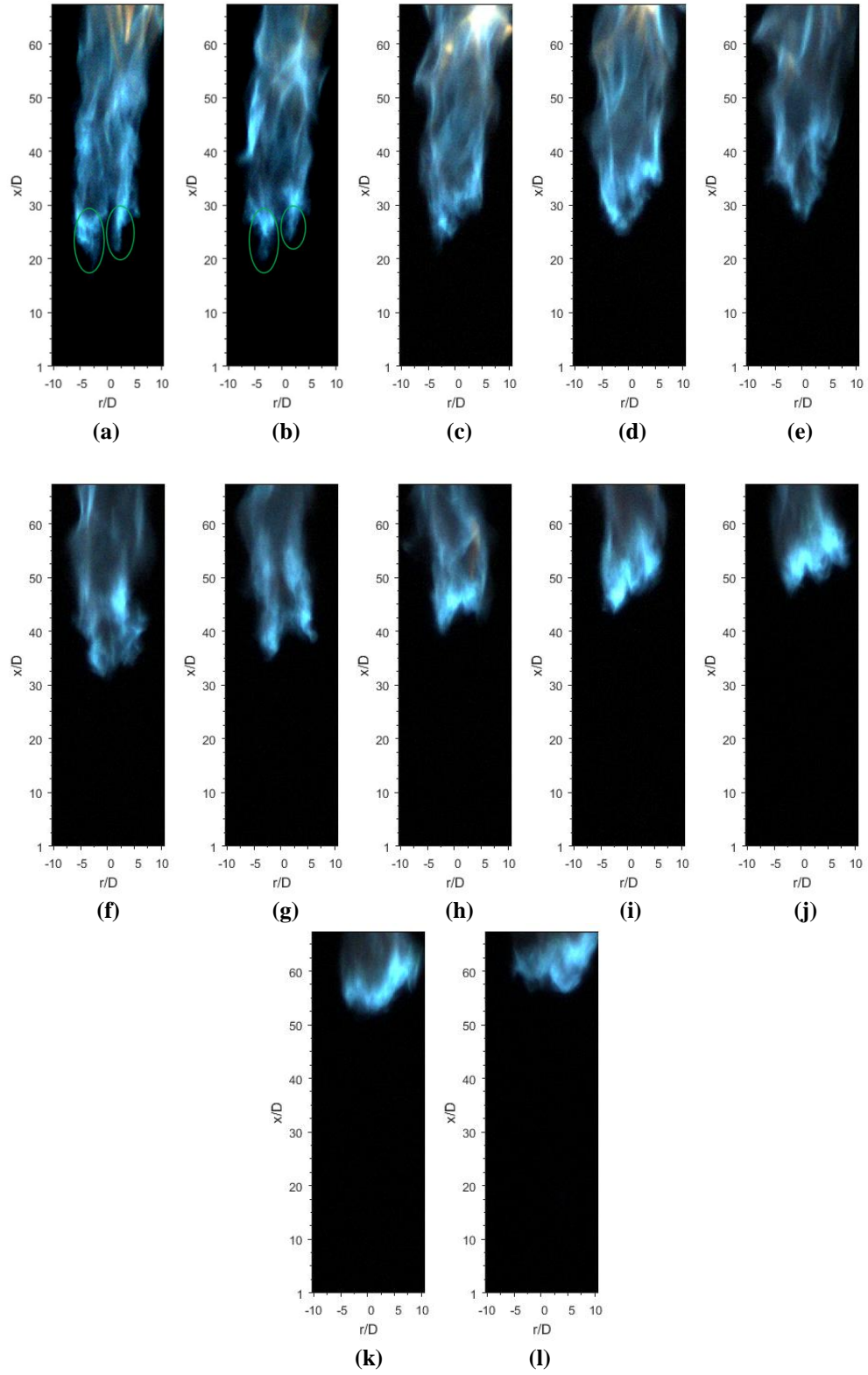


Figure 21: Image Sequence showing blowout of the jet flame, i.e., Mode B. The images shown here are of successive frames recorded at a rate of 60 frames per second.

Figure 21(a-i) illustrates a typical image sequence during flame blowout (Mode B) and Figure 22(a – i) shows a binary image sequence of the same blowout occurrence in order to highlight the flame edges. The temporal resolution between the images in these sequences is 0.0167 seconds (1/60). The onset of avalanche flame-base motion is identified as the frame after which the downstream motion of the flame base occurs for more than 0.067 seconds (4 frames). This threshold duration was determined from observing the fluctuation durations in Mode A, where the flame base retracted from its upstream propagation within 4 frames.

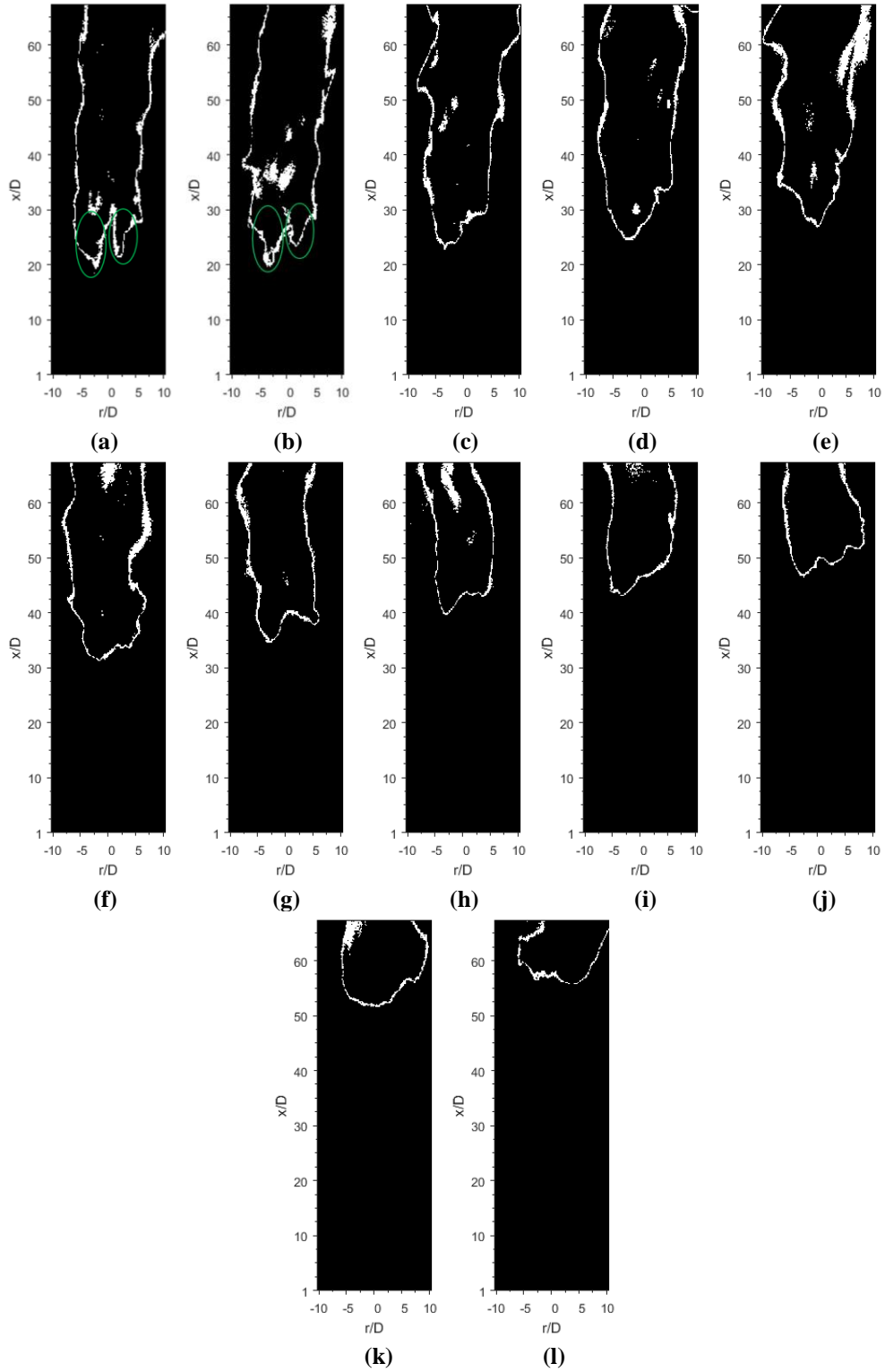


Figure 22: Binary image sequence of Mode B, which clearly shows the extinction of a leading edge flame stem at the start of the blowout process. This binary image sequence corresponds to the sequence shown in Figure 21.

Figure 21(b) and Figure 22(b) are the last frames when the flame exhibited “Mode A” behavior, where we can observe the two stems at the flame base (in Figure 22((a) and (b)) that indicate the presence of edge flame propagation [19] [16]. Figure 21(c) and Figure 22(c) are the first frames of avalanche downstream motion. It can be observed that the two stems observed in Figure 21((a) and (b)) and Figure 22((a) and (b)) are absent in Figure 21(c) and Figure 22(c). Thus, it appears that the onset of the avalanche downstream motion is always preceded by the extinction of the stems. Interestingly, previous works on classical turbulent lifted flames also showed that the extinction of edge flame stems preceded the onset of flame blowout [3] [43]. Whether the extinction of flame stems is the actual trigger mechanism for flame blowout sequence is not clear from our flame luminosity imaging. In the subsequent frames Figure 21(c-l), the flame moves $\approx 35 D$ downstream (186 mm). The flame base appears more intense in Figure 21(h-k). At this downstream location, the entrainment of ambient air may be causing the formation of multiple reaction zones due to increased fuel/oxidizer mixing, and this could be the cause for the intense appearance of the flame base, as suggested by Dally et al. [44]. We also observe that towards the end of the blowout sequence, the flame base appears to be wider than it was at the start of the image sequence, i.e. when the flame was still executing Mode A motions. This is consistent with the observations of Han and Mungal [9] on a classical turbulent lifted flame at near blowout conditions. Figure 21(l) is the last frame where the flame base was within the measurement field of view ($x/D < 68.5$) and this is followed by a global flame extinction. The similarities in our observations of Mode B with previous studies on blowout in conventional turbulent lifted

flames suggests that the blowout mechanism may not be significantly different for jet flames in a vitiated coflow.

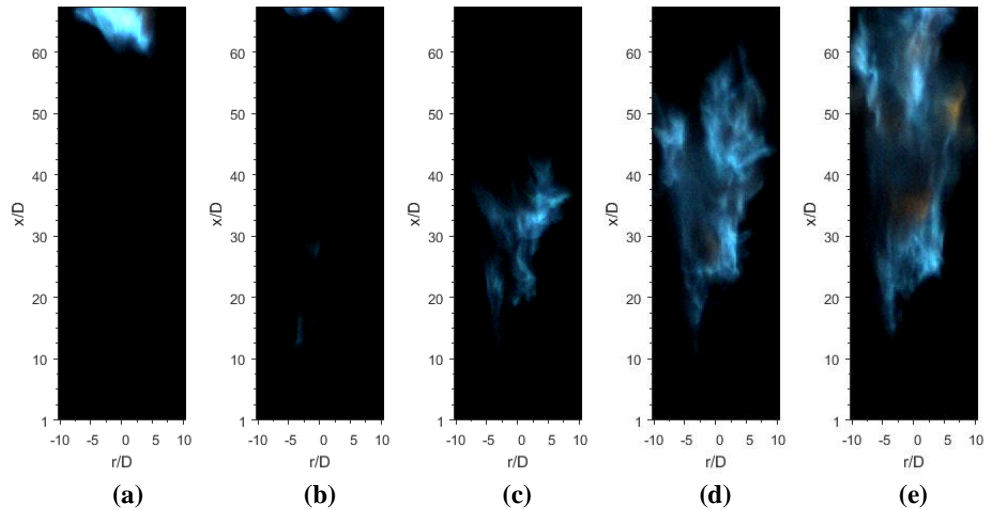


Figure 23: Image sequence illustrating the relight sequence of the jet flame succeeding an occurrence of blowout (Mode B).

The chief difference, however, in jet flame blowout in a heated or vitiated coflow lies in the fact that after occurrence of blowout, the flame is lit once again. The global flame extinction is followed by a relight sequence involving the formation and growth of a new autoignition kernel, as shown in Figure 23. The newly lit flame then proceeds to execute Mode A, B or C.

3.1.3 Autoignition Kernel Formation and Flame Re-anchor (Mode C)

During several realizations of avalanche downstream flame-base motion, we observed the formation and growth of autoignition kernels at a location significantly upstream of the lifted flame base, i.e., much closer to the jet exit. These kernels propagate downstream and

re-anchor the flame, preventing complete blowout. Occurrences of this mode can be seen from the temporal evolution of liftoff height in Figure 19- the liftoff height of the flame base increases but is brought back down before reaching the relatively higher values that indicate blowout. It is immediately evident that Mode C serves to enhance the stabilization of the lifted jet flame by preventing the execution of the unstable Mode B.

Figure 24 (a-j) shows an image sequence of flame motion and the formation/evolution of autoignition kernels. Figure 24(a) shows an image where the downstream flame motion has just started. Similar to the flame blowout sequence shown in Figure 22, the two flame stems about the jet centerline that indicate edge flames are absent in Figure 24. Further, with increasing downstream displacement, the flame base appears more intense similar to Mode B. When the flame base has motion downstream about $30D$, an autoignition kernel appears at $x/D \approx 7.5$ (Figure 24 (g)). The autoignition kernel grows rapidly between Figure 24(g-i); during this time, there is also a continued downstream motion of the flame base. The rapidly growing autoignition kernel “catches up” with the flame base in Figure 24(j) and prevents the flame from completing the global extinction (Mode B). The re-anchored flame base, just after its interactions with autoignition kernel, is located at $x/D \approx 10$. Subsequent to re-anchoring, the flame may be stabilized for a while (executing “Mode A” type motions) or undergo another avalanche downstream motion that may lead to blowout (Mode B) or re-anchoring from autoignition kernels (Mode C).

With the delineation of the different dominant flame base motions, it is evident that autoignition is responsible for stabilizing the flame in Mode C and no stabilization

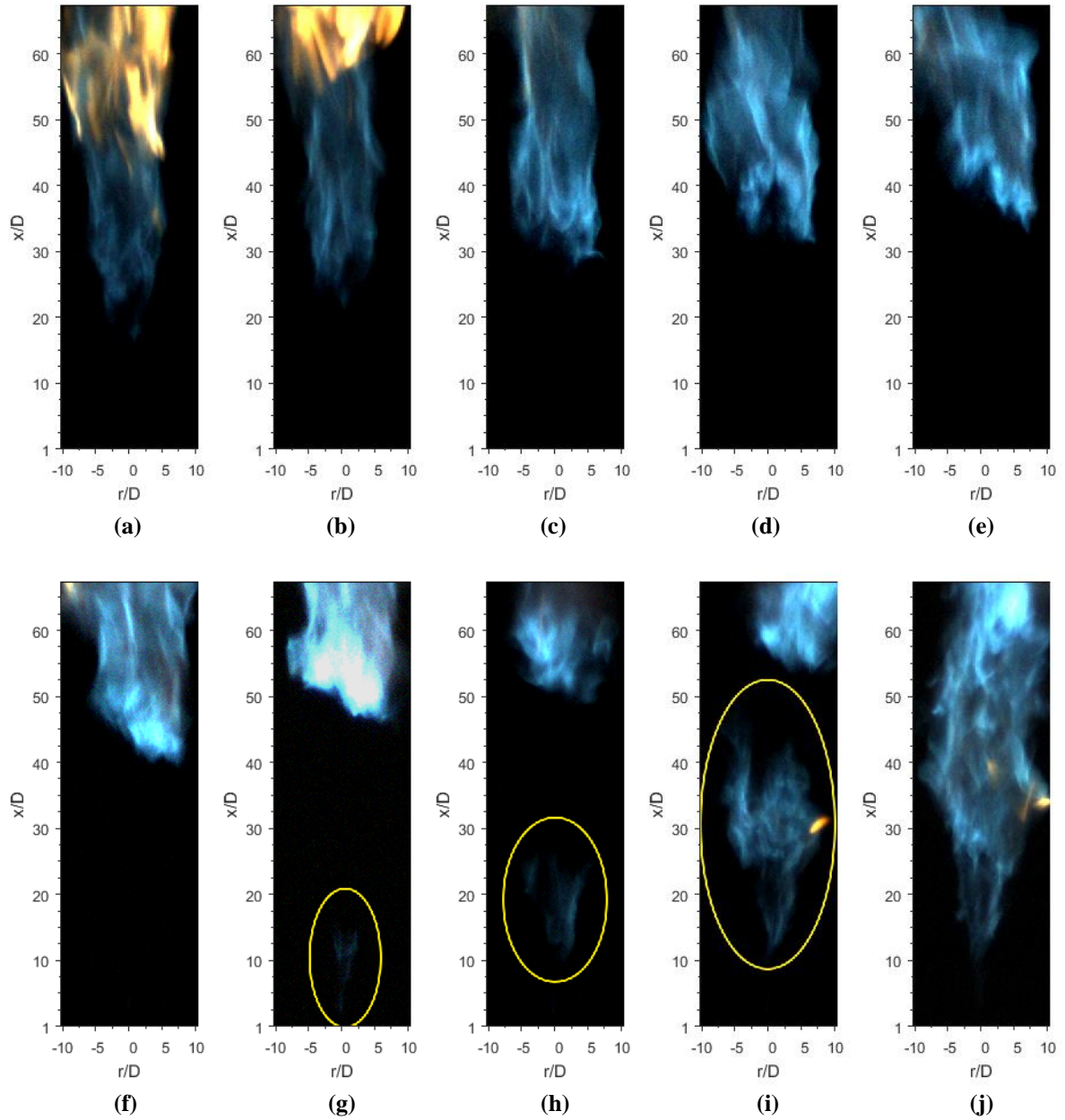


Figure 24: Image sequence demonstrating the formation of ignition kernels and the subsequent re-anchoring of the lifted jet flame.

mechanism is active during Mode B. Therefore, to further investigate the dominant stabilization mechanism in jet flames, our focus now lies on Mode A flame motions. Nevertheless, it is also essential to understand the behavior of the other modes in order to completely understand the phenomena occurring here. The discussion on the three flame modes leads to several questions that arise regarding their characteristics and causative mechanisms:

1. What is the contribution of autoignition vs. partial premixing towards flame stabilization during Mode A motions?
2. How do the flow conditions like jet exit Reynolds number, O_2 mole fraction, and co-flow temperature influence the predominant modes that the flame will execute?
3. What mechanisms trigger the transition from Mode A to Mode B and C? What flow conditions influence the formation of autoignition kernels?

In the following sections, we find qualitative answers to questions 1 and 2 using observations of flame base statistics complemented by kinetics simulations.

3.2 Contribution of Autoignition vs. Partial Premixing in Mode A Motions

At this point in our discussion, it is worth noting that in a study by Arndt et al. [45] on autoignition of a pulsed CH_4 jet in a vitiated coflow produced by a H_2/Air flame, it was

observed that for many of the test cases, the height of formation of the first ignition kernel was greater than the average liftoff height of the flame. This indicated that the flame base was moving further upstream after the formation of the autoignition kernel, leading to the conjecture that there may be a possibility of occurrence of secondary ignition events. Whereas their measurement of liftoff height was the average of steady flame liftoff height taken over 10ms for each ignition event, our definition of liftoff height is the average of the flame liftoff height taken over 25 seconds. Therefore, it is not possible to make a direct comparison with their observations. However, we did observe formation of ignition kernels over a range of axial positions, extending both above and below the time averaged flame liftoff height. While the role of autoignition in Mode C is abundantly clear, this observation leads us to consider the possibility that after the flame is re-anchored by Mode C, the Mode A motions that follow may indeed be influenced by rapid ignition kernel formation at lower axial positions. The sudden upstream motion of the flame base observed in Mode C in turn moves the high temperature zone upstream. Thermal expansion at this new stabilization zone could reduce local strain rates, facilitating ignition of oncoming reactants in fuel lean mixtures. Therefore, with a view to testing this hypothesis, we made use of chemical kinetic simulations to compute chemical time scales for autoignition in order to further investigate the significance of autoignition as a mechanism of flame stabilization.

3.2.1 Chemical Kinetics Results

Chemical kinetics simulations were performed using Cantera [46] to provide depth to the discussion on chemical time scales (liftoff heights) in Mode A stabilized flames. The chemical kinetic mechanism used by the Cantera source code that we employed was GRI Mech 3.0 [47]. This mechanism involves 53 species and 325 reactions. It is optimized for combustion of natural gas and is widely used for kinetic simulations of methane combustion. The ignition time of several homogeneous CH_4/Air mixtures was estimated at atmospheric pressure and at different oxygen mole fractions and mixture temperatures to provide an

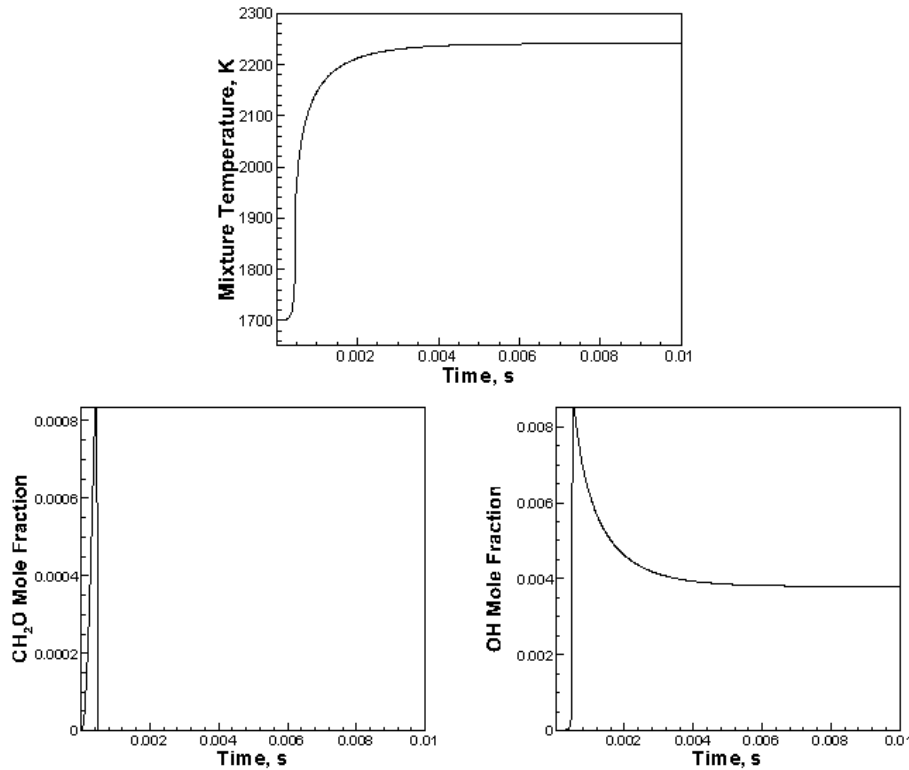


Figure 25: Sample plot illustrating the evolution of temperature, CH_2O mole fraction and OH mole fraction. This plot corresponds to the simulated case with a mixture temperature of 1700 K and $X_{O_2} = 7.39\%$.

estimate of shortest time delay for kernel formation. Figure 25 shows a sample series of plots containing the temporal evolution of mixture temperature, CH_2O mole fraction and OH mole fraction. The time at which the peak of the OH mass fraction occurred was taken to be the ignition delay time. An order of magnitude comparison of these time scales helps to unravel the contribution of autoignition against that of partially premixed stabilization.

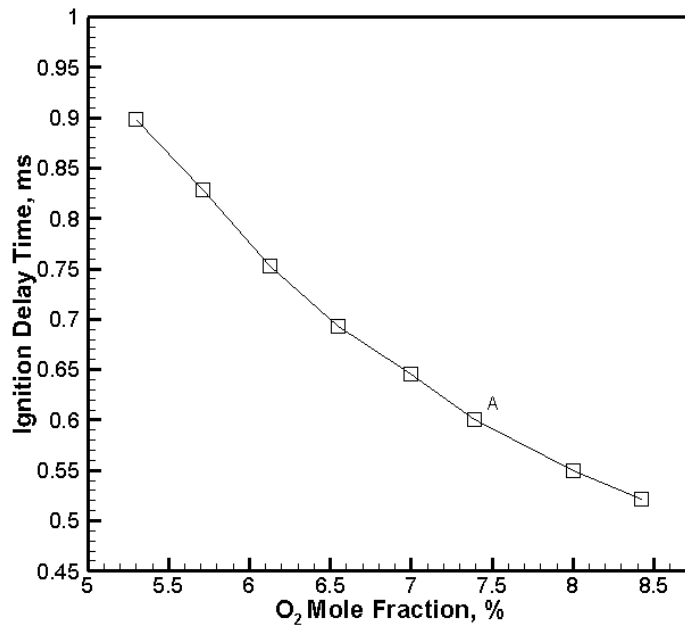


Figure 26: Ignition delay time computed by Cantera for a range of oxygen mole fractions. The temperature of the homogeneous mixture was set at 1705 K.

Here, we consider the vitiated coflow case with $\phi = 0.625$ at a jet Reynolds number of 4500 (Flame #5, Table 1). The average liftoff height for this case is 109 mm and the fuel jet centerline velocity is 20.3 m/s. Assuming the characteristic flow velocity to be jet centerline exit velocity, this average liftoff height translates to a convective time scale of ~ 5 ms. By comparison, the time scale calculated based on the velocity of the lifted CH_4/Air flame base,

as calculated by Watson et al. [11], is ~92 ms and the time scale based on stoichiometric velocity, as calculated by Han and Mungal [10], is ~101 ms.

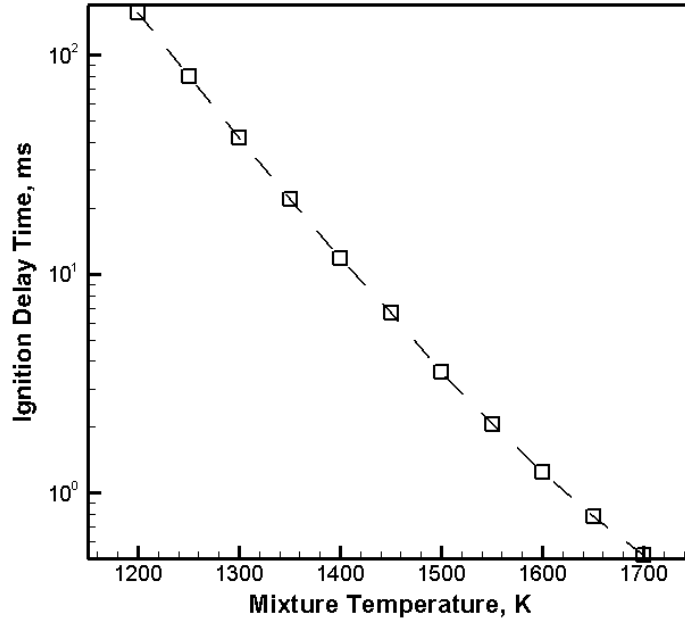


Figure 27: Logarithmic scale plot of ignition delay time of a homogeneous CH_4/Air mixture at atmospheric pressure and $X_{O_2}=7.39\%$ computed by Cantera for a range of starting fuel-oxidizer mixture temperatures.

Now, from Figure 26, the ignition time delay of a homogeneous mixture with the same O_2 mole fraction as our experimental test case (marked A) is 0.6 ms. It can therefore be seen that the ignition kernel formation occurs at a time scale that is an order of magnitude shorter than the flow convective time-scale corresponding to the flame base. However, it must be noted that the homogeneous mixture computations represents the shortest possible chemical time-scale for kernel formation. Echehki & Chen [48] stated that compared to homogeneous mixtures, the ignition delay time increases by a factor of two or more in a turbulent

environment due to heat losses and radical losses caused by turbulent mixing. Even with this increase in delay time, the flow convective time-scales are still commensurate with, if not considerably greater than the autoignition kernel formation timescales. At a mixture temperature of 1475 K (the lowest coflow adiabatic flame temperature in our test matrix (Table 1)) and $X_{O_2} = 7.39\%$, the ignition delay time is ~ 6 ms which is of an order comparable to the convective time scales of the Mode A stabilized flames. Hence, we expect a substantial contribution (if not dominant contribution) from autoignition kernels towards flame stabilization in this region.

Extending the chemical kinetics simulations at $X_{O_2} = 7.39\%$ to mixture temperatures lower than the coflow adiabatic flame temperatures of the range of cases that we experimentally tested revealed an exponential increase in ignition delay time with decrease in mixture temperature, illustrated by a logarithmic scale plot in Figure 27. At the higher mixture temperatures shown in this plot, it can be seen from the earlier discussion that notwithstanding the delaying effects of turbulent mixing, the ignition delay times of the homogeneous mixtures in turbulent environments are still within contention for autoignition kernel formation to dominate the flame stabilization process. However, considering the exponential increase in ignition delay time as we go to lower temperatures, the effects of turbulence are expected to be substantial on the formation of autoignition kernels. Turbulence, as a phenomenon, is inherently related to unsteadiness and fluctuations. Since autoignition requires the formation of homogeneous mixtures, i.e. a region of spatially uniform thermochemical conditions, the fluctuations caused by turbulence serve to hinder

kernel formation, despite enhancing mixing. Thus, compounded with the very high ignition delay times, we expect the role of autoignition to diminish in turbulent environments at low temperatures.

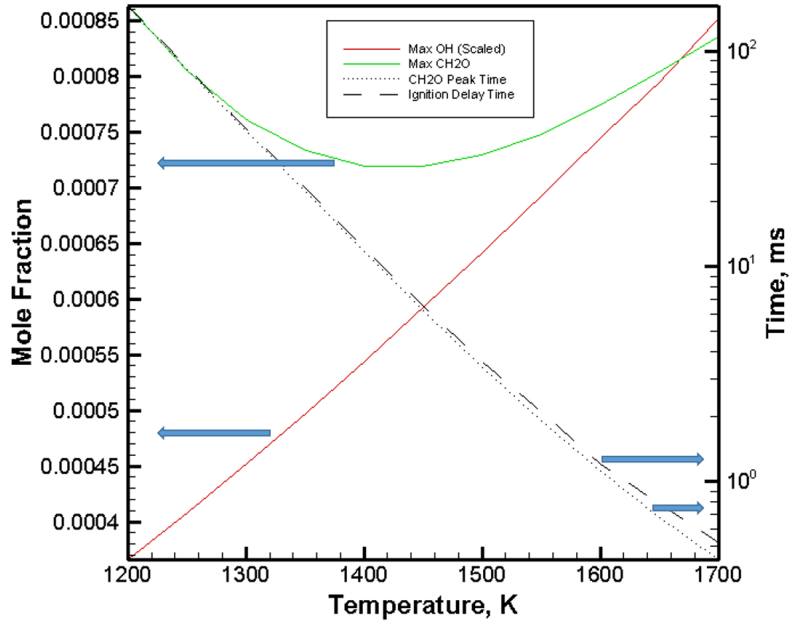


Figure 28: Change in ignition delay time, maximum OH and CH_2O mole fractions and CH_2O peak time with mixture temperature, plotted for a homogeneous CH_4/Air mixture at $X_{O_2} = 7.39\%$. The OH mole fraction is scaled down by a factor of 10.

Figure 28 shows that the time at which CH_2O mole fraction peaks is very closely followed by the ignition delay time. This is consistent with the nature of CH_2O as a precursor in the ignition of CH_4/Air mixtures. While the maximum OH mole fraction is seen to vary linearly with mixture temperature, it is interesting to note a minimum in the maximum CH_2O mole fraction at temperature near $T = 1400 K$. This trend was observed at all three cases of X_{O_2} mentioned in Table 1 (7.39%, 8.42% and 9.98%), as shown in Figure 29. Above this

temperature, we see that in addition to ignition delay times being comparable with flow convective time scales, the occurrence of increasing CH_2O peaks with temperature indicates a strong contribution from autoignition in flame stabilization. The increase in CH_2O as the temperature decreases below 1400 K indicates the formation of ignitable mixtures, but as discussed earlier, we expect that the effect of turbulence is to significantly delay the ignition process.

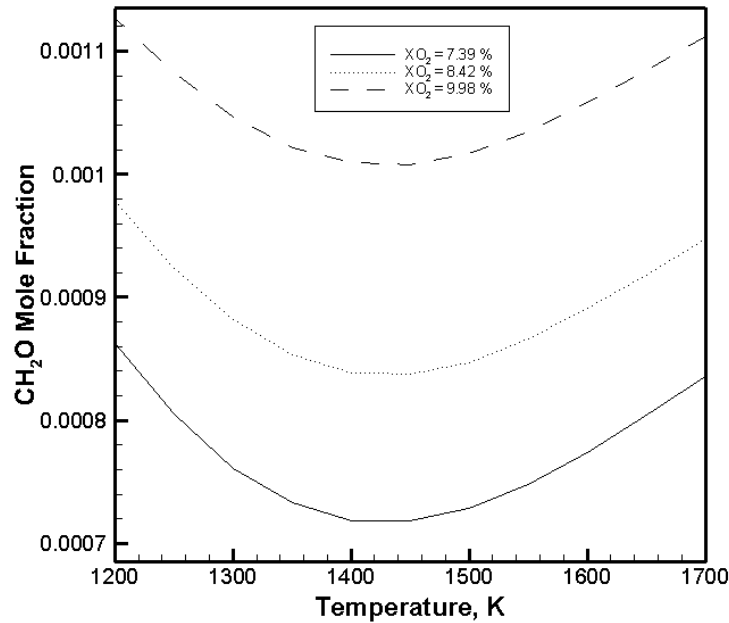


Figure 29: Minima in maximum CH_2O mole fraction observed at similar mixture temperature for three different values of X_{O_2}

A study performed using CH^* -chemiluminescence on lifted natural gas jet flames by Medwell & Dally [49] found that with increase in coflow temperature from 1100 K to 1600 K and oxygen mole fraction from 3% to 12%, the change in liftoff height was not monotonic. It is very interesting to note that for the $X_{O_2} = 3\%$ case, they saw an increase in liftoff height

with increase in temperature until $T = 1400$ K. After this point, with increase in temperature, the liftoff height decreased. Juxtaposing their observation with the trend illustrated in Figure 29, we conjecture that this could signify a transition region where the dominance of autoignition as the flame stabilization mechanism may diminish.

3.3 Other Observations from Experiments

An interesting observation from our experiments was made at the test case where the coflow adiabatic flame temperature was 1475 K and $X_{O_2} = 7.36\%$. This was observed to result in a case of flameless oxidation. A very faint outline of the jet flame was visible to the naked eye and could not be captured by our camera.

A further decrease in X_{O_2} at this temperature would increase the ignition time delay, as can be inferred from Figure 26. At an experimental case we tested with $X_{O_2} = 4.26$ and $Re_D = 4500$, yet another interesting observation was made. The flame did not stabilize at all, i.e., there was no bulk jet flame. The formation of autoignition kernels was observed. However, these kernels were formed at locations far downstream from the burner jet. Under highly oxygen rich conditions, the formation of homogeneous mixtures was thus seen to take considerably longer time, leading to the large downstream shift in the position of ignition kernel formation. A closer inspection of the images suggested that this case could be in the ‘Random Spots’ regime suggested by Markides & Mastorakos [50], which they described as follows - “Independent kernels appeared and were advected with the flow before they disappeared.” Figure 30 shows an instance of the flame in ‘Random Spots’ regime. In the

higher jet velocity case ($Re_D = 8000$), however, instances of the jet flame exhibiting Mode A motions were observed. A regime map of these cases is presently being delineated in our lab.

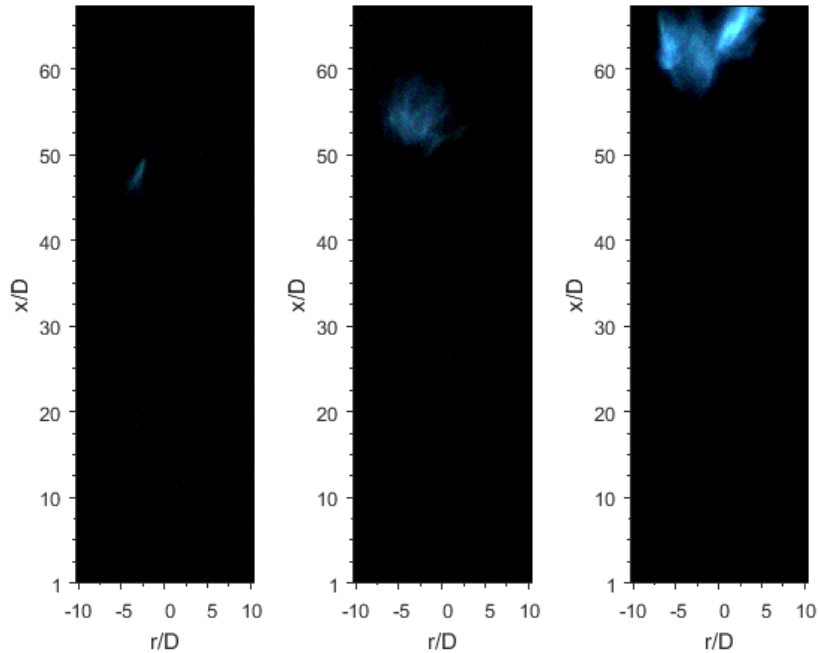


Figure 30: Random Spots' regime observed at jet Reynolds number of 4500, coflow adiabatic flame temperature of 1475 K and at 4.26% O_2 mole fraction.

3.4 Influence of Aero/thermochemical Properties on Flame Stabilization

The role of different aero/thermochemical properties, namely, jet-exit Reynolds number, O_2 mole fraction, and coflow temperature, on favoring/inhibiting different modes of flame base motion was examined. Figure 31 shows the percentage of realizations that corresponded to the different flame modes. All the configurations in the test matrix consistently exhibited the dominance of Mode A over the other two modes observed in the flames.

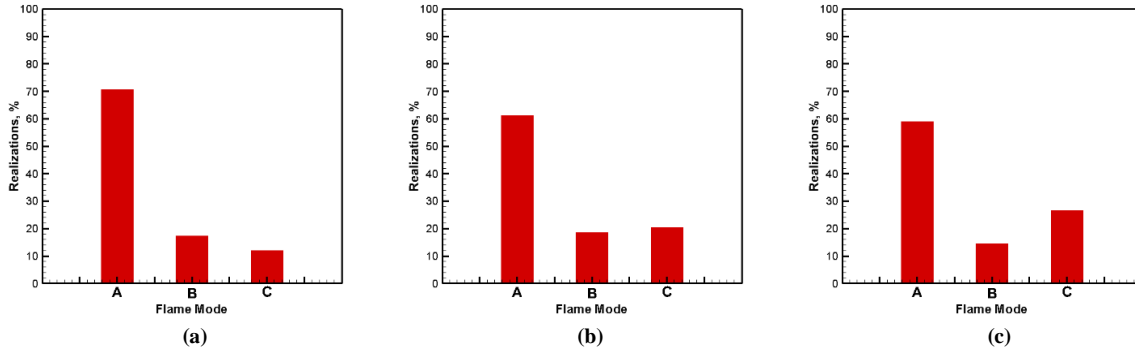


Figure 31: Flame mode percentages compared for three cases: (a) $\Phi = 0.5, Re_D = 4500$, (b) $\Phi = 0.575, Re_D = 4500$, and (c) $\Phi = 0.575, Re_D = 8000$.

Figure 31((a) and (b)) shows that the occurrence of Mode C is higher at greater temperatures. This is an expected observation because at identical turbulence conditions, the formation of autoignition kernels is dependent on the local temperature, once homogeneous regions have been formed. However, it must be noted that since there is an increase in the equivalence ratio, there is also a decrease in the O_2 mole fraction in (b). Figure 33 and Figure 32 show the temporal evolution of temperature, CH_2O mole fraction and OH mole fraction based on chemical kinetic simulations performed for homogeneous CH_4/Air mixtures with starting temperature and X_{O_2} corresponding to the cases depicted in Figure 31(a) and Figure 31(b) respectively. Taking the peak in OH to indicate ignition delay time, it is clear that ignition is faster at $T = 1615 K, X_{O_2} = 8.42\%$. This is consistent with the observation of higher occurrence of Mode C for this case, as shown in Figure 31(b). However, a comparison of the CH_2O evolutions reveals that the peak mole fraction is higher at $T = 1475 K, X_{O_2} = 9.98\%$.

Thus, despite the stronger presence of an autoignition precursor, temperature appears to be the determining factor which causes higher occurrences of Mode C.

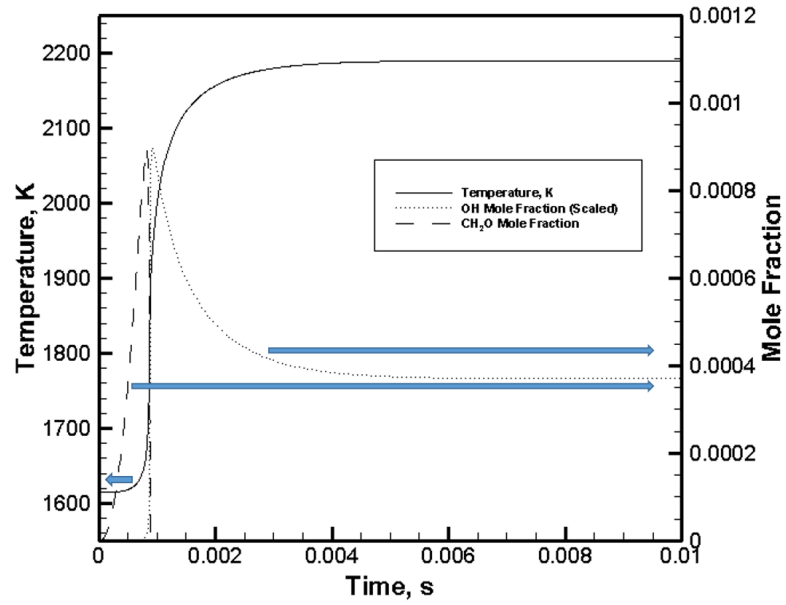


Figure 32: Temporal evolution of temperature, CH_2O mole fraction and OH mole fraction (scaled down to match the peak in CH_2O) for a homogeneous CH_4/Air mixture at a starting temperature of 1615 K and $X_{O_2} = 8.42\%$

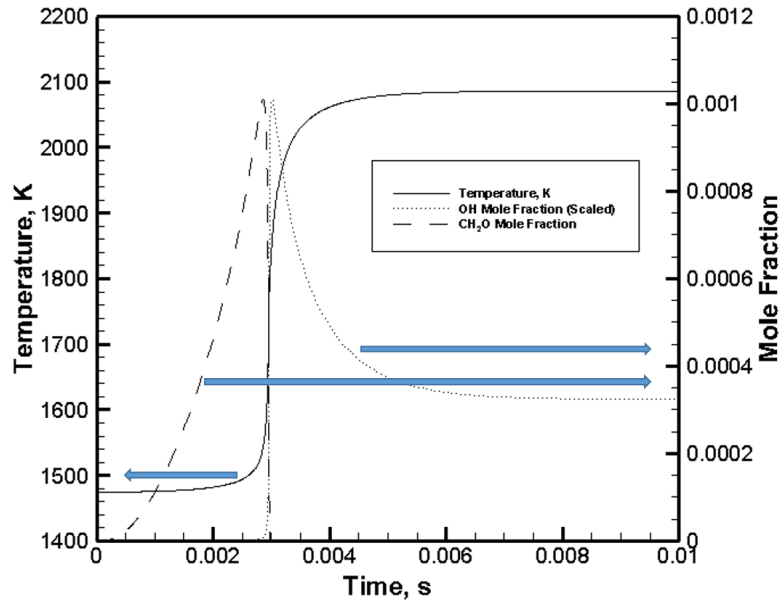


Figure 33: Temporal evolution of temperature, CH_2O mole fraction and OH mole fraction (scaled down to match the peak in CH_2O) for a homogeneous CH_4/Air mixture at a starting temperature of 1475 K and $X_{O_2} = 9.98\%$

A comparison between Figure 31((b) and (c)) also reveals that autoignition (Mode C) plays a relatively stronger part in flame stabilization at higher turbulence conditions. Further, it can be observed that increasing jet Reynolds number causes a decrease in the occurrence of Mode B (complete blowout), while keeping the percentage realization of Mode A approximately the same. This shows that increase in turbulence levels favors the formation of autoignition kernels, presumably because of the faster mixing of fuel and oxidizer stream. It is important to note at this point that this could depend on the Re_D values that we have studied. While Markides & Mastorakos [20] suggested that turbulence has a delaying effect on autoignition (they increased turbulence by increasing the coflow air velocity) and Echehki & Chen [48] explained the delayed autoignition times in turbulent environments, Oldenhof et

al. [26] showed a decrease in flame lift-off height with increasing Reynolds number between 3000 and 5000 but an increase in lift-off height when the Reynolds number was between 5000 and 9500. Hence, the dependence of autoignition on turbulence and how its role as a dominant flame stabilization mechanism varies with turbulence levels is not yet completely understood. We seek to uncover these trends in future studies.

4 CONCLUSIONS

4.1 Concluding Remarks

Experimental studies of a non-premixed CH_4 jet in a vitiated coflow of hot combustion products have been reported in this manuscript. Previous studies on turbulent fuel jets in high temperature coflow have described the structure of the lifted jet flames and studied the unsteadiness in their nature. These have led to further research that has attempted to identify the flame stabilization mechanisms active in turbulent lifted jet flames in vitiated coflow. Our work was performed with the objective to gain a deeper understanding the global features and characteristic behavior of jet flames in this configuration and further, to contribute to the existing knowledge regarding flame stabilization mechanisms and attempt to identify the dominant mechanism that sustains the flame. The results from our studies point to the following major inferences:

- Three distinct flame modes (stable flame base, complete blowout, autoignition re-anchoring) are exhibited by turbulent jet flames issuing into a vitiated coflow. All three modes are found to occur across every configuration, with the exception of the case which fell in the '*Random Spots*' regime. The occurrence of the three modes did not follow an observable pattern, pointing to the unsteadiness and intermittency of the turbulent flow field. Flame mode statistics reveal that the most dominant of these modes is the stable flame base mode (Mode A).

- The global chemical time scales are considerably lower in vitiated coflow cases when compared to cold coflow cases during stable combustion mode (Mode A). Since Mode B is an unstable mode and flame stabilization via re-anchoring is clearly effected by autoignition in Mode C, we focused on identifying the dominant flame stabilization mechanism active in Mode A. Furthermore, considering that Mode A is the most frequently occurring of the three modes, it followed that an investigation of Mode A would shed light on the overall picture regarding dominant stabilization mechanism(s) in lifted jet flames in vitiated coflow. The visually observed flame structure of the jet flame during Mode A exhibited similarities with the structure of leading edge flames that have previously been observed and widely studied in conventional or classical lifted turbulent jet flames. Even though this led us to hypothesize that partially premixed flame propagation may be the dominant flame stabilization mechanism in Mode A, chemical kinetic simulations reveal that autoignition is an active mechanism involved in sustaining Mode A and suggest that it may be dominant compared to partially premixed propagation. However, this is seen to be dependent on the coflow temperature, and further studies will have to be performed before conclusive statements can be made in this regard.
- The role of increasing turbulence levels (higher jet exit Reynolds number) appears to favor a quicker formation of autoignition kernels that prevents complete blowout in many instances. However, increasing the jet Reynolds number had no effect on the fraction of realizations exhibiting stable flame base mode. In the case of

turbulent non-premixed flames, there is constant interplay between turbulence and chemistry. Therefore, establishing a simplistic relationship between turbulence and its effect on the formation of autoignition kernels is difficult. To understand how changing turbulence levels affects flame stabilization, we must extend our study to a wider range of Reynolds numbers.

4.2 Future Work

The results presented in this thesis and the discussion thereof point toward a considerable need for further research to better understand flame stabilization mechanisms active in lifted jet flames in vitiated coflow. Having obtained a picture of the global features of these flames, the next natural step is to focus on the local features and obtain detailed measurements. Some of the major points of focus in our future research will be:

- Obtaining local velocity field measurements at the base of the lifted flame, in order to investigate the role of large scale vortices on stabilization. Further, a look into local extinctions caused by vortical structures at the edge flames just downstream of the stabilization point will augment our efforts into understanding the motions of the flame base.
- We will also perform simultaneous imaging of the flow field temperature and concentrations. Pertinent observations can be made based on the temporal and spatial distribution of important radicals in hydrocarbon combustion, such as OH , CH and

CH_2O . In methane flames, CH_2O radical pool buildup has been reported as a precursor to autoignition. Our measurements will look for the occurrence of such radical pools at lower coflow temperatures with the aim of understanding the influence of autoignition under such conditions.

- We will also look to obtain time resolved simultaneous measurements of heat release rate, mixture fraction and scalar dissipation rate in order to experimentally confirm the predominantly DNS based observation that autoignition kernels form at regions of low scalar dissipation. Mapping the kernel formation and flame propagation histories in mixture fraction space will add depth to ongoing research and discussions on the topic of autoignition in jet flames in vitiated coflow.
- Lastly, we plan to extend our studies on this flame configuration to alternate fuels such as dimethyl ether (DME). DME possesses the property of multi-stage ignition and has interesting low temperature chemistry; it produces combustion radicals at much lower coflow temperatures. Also, given the slow chemical time scales of DME ignition (low Damkohler number), we expect the effects of turbulence to gain higher prominence than in the case of CH_4 . Due to its low emissions and abundant availability, DME is a strong candidate to replace diesel as fuel in automotive engines of the future, and is therefore our chosen bio-fuel for further research.

5 REFERENCES

- [1] C. Burgess and C. Lawn, "The premixture model of turbulent burning to describe lifted jet flames," *Combustion and Flame*, vol. 119, pp. 95-108, 1999.
- [2] W. Pitts, "Assessment of theories for the behavior and blowout of lifted turbulent jet diffusion flames," *Proceedings of the Combustion Institute*, vol. 22, pp. 809-816, 1988.
- [3] K. Lyons, "Toward an understanding of the stabilization mechanisms of lifted turbulent jet flames: Experiments," *Progress in Energy and Combustion Science*, vol. 33, pp. 211-231, 2007.
- [4] C. J. Lawn, "Lifted flames on fuel jets in co-flowing air," *Progress in Energy and Combustion Science*, vol. 35, pp. 1-30, 2009.
- [5] K. Wohl, N. Kapp and C. Gazley, "The stability of open flames," *Symposium on Combustion and Flame, and Explosion Phenomena*, vol. 3, pp. 3-21, 1948.
- [6] L. Vanquickenborne and A. Van Tiggelen, "The stabilization mechanism of lifted diffusion flames," *Combustion and Flame*, vol. 10, pp. 59-69, 1966.
- [7] G. Kalghatgi, "Lift-off Heights and Visible Lengths of Vertical Turbulent Jet Diffusion Flames in Still Air," *Combustion Science and Technology*, vol. 41, pp. 17-29, 1984.
- [8] E. Hasselbrink Jr. and M. Mungal, "Characteristics of the velocity field near the instantaneous base of lifted non-premixed turbulent jet flames," *Symposium (International) on Combustion*, vol. 27, pp. 867-873, 1998.
- [9] D. Han and M. Mungal, "Observations on the Transition from Flame Liftoff to Flame

- Blowout," *Proceedings of the Combustion Institute*, vol. 28, pp. 537-543, 2000.
- [10] D. Han and M. Mungal, "Simultaneous measurements of velocity and CH distributions. Part 1: jet flames in co-flow," *Combustion and Flame*, vol. 132, p. 565–590, 2003.
- [11] K. A. Watson, K. M. Lyons, J. M. Donbar and C. D. Carter, "Scalar and Velocity Field Measurements in a Lifted CH₄–Air Diffusion Flame," *Combustion And Flame*, vol. 117, pp. 257-271, 1999.
- [12] L. Muñiz and M. Mungal, "Instantaneous flame-stabilization velocities in lifted-jet diffusion flames," *Combustion and Flame*, vol. 111, pp. 16-30, 1997.
- [13] N. Peters and F. Williams, "Liftoff Characteristics of turbulent jet diffusion flames," *AIAA Journal*, vol. 21, pp. 423-429, 1983.
- [14] N. Peters, "Local quenching due to flame stretch and non-premixed turbulent combustion," *Combustion Science and Technology*, vol. 30, pp. 1-17, 1983.
- [15] N. Peters, *Turbulent Combustion*, Cambridge: Cambridge University Press, 2000.
- [16] J. Buckmaster and R. Weber, "Edge-flame-holding," in *Symposium (International) on Combustion*, 1996.
- [17] C. Müller, H. Breitbach and N. Peters, "Partially premixed turbulent flame propagation in jet flames," in *Symposium (International) on Combustion*, Irvine, 1994.
- [18] G. Ruetsch, L. Vervisch and A. Linan, "Effects of heat release on triple flames," *Physics of Fluids*, vol. 7, pp. 1447-1454, 1995.
- [19] J. Buckmaster, "Edge Flames," *Progress in Energy and Combustion Science* 28, pp.

- 438-475, 2002.
- [20] K. Watson, K. Lyons, J. Donbar and C. Carter, "Simultaneous Rayleigh imaging and CH-PLIF measurements in a lifted jet diffusion flame," *Combustion and Flame*, vol. 123, pp. 252-265, 2000.
- [21] K. Watson, K. Lyons, J. Donbar and C. Carter, "Observations on the leading edge in lifted flame stabilization," *Combustion and Flame*, vol. 119, pp. 199-202, 1999.
- [22] R. Miake-Lye and J. Hammer, "Lifted turbulent jet flames: A stability criterion based on the jet large-scale structure," *Symposium (International) on Combustion*, vol. 22, pp. 817-824, 1989.
- [23] J. Kelman, A. Eltobaji and A. Masri, "Laser Imaging in the Stabilisation Region of Turbulent Lifted Flames," *Combustion Science and Technology*, vol. 135, pp. 117-134, 1998.
- [24] K. M. Lyons, K. A. Watson, C. D. Carter and J. M. Donbar, "On flame holes and local extinction in lifted-jet diffusion flames," *Combustion and Flame*, vol. 142, pp. 308-313, 2005.
- [25] R. Cabra, J. Y. Chen, R. W. Dibble, A. N. Karpetsis and R. S. Barlow, "Lifted methane-air jet flames in a vitiated coflow," *Combustion and Flame*, vol. 143, pp. 491-506, 2005.
- [26] E. Oldenhof, M. J. Tummers, E. H. van Veen and D. J. E. M. Roekaerts, "Ignition kernel formation and lift-off behaviour of jet-in-hot-coflow flames," *Combustion and Flame*, vol. 157, pp. 1167 - 1178, 2010.

- [27] S. Lamige, K. Lyons, C. Galizzi, M. Kuhni, E. Mathieu and D. Escudie, "Lifting and splitting of nonpremixed methane/air flames due to reactant preheating," *Combustion Science and Technology*, 2015.
- [28] C. Yoo, E. Richardson, R. Sankaran and J. Chen, "A DNS study on the stabilization mechanism of a turbulent lifted ethylene jet flame in highly-heated coflow," *Proceedings of the Combustion Institute*, vol. 33, pp. 1619-1627, 2011.
- [29] A. R. Masri, R. Cao, S. B. Pope and G. M. Goldin, "PDF calculations of turbulent lifted flames of H₂/N₂ fuel issuing into a vitiated co-flow," *Combustion Theory and Modelling*, vol. 8, pp. 1-22, 2004.
- [30] R. Cabra, T. Myhrvold, J.-Y. Chen, R. W. Dibble, A. N. Karpetis and R. S. Barlow, "Simultaneous Laser Raman-Rayleigh-Lif Measurements And Numerical Modeling Results Of A Lifted Turbulent H₂/N₂ Jet Flame In A Vitiated Coflow," *Proceedings of the Combustion Institute*, vol. 29, pp. 1881 - 1888, 2002.
- [31] E. Mastorakos, "Ignition of turbulent non-premixed flames," *Progress in Energy and Combustion Science*, vol. 35, pp. 57-97, 2009.
- [32] C. Yoo, R. Sankaran and J. Chen, "Three-dimensional direct numerical simulation of a turbulent lifted hydrogen jet flame in heated coflow: flame stabilization and structure," *Journal of Fluid Mechanics*, vol. 640, pp. 453-481, 2009.
- [33] R. Gordon, A. Masri, S. Pope and G. Goldin, "A numerical study of auto-ignition in turbulent lifted flames issuing into a vitiated co-flow," *Combustion Theory and Modelling*, vol. 11, pp. 351-376, 2007.

- [34] R. Gordon, A. Masri, S. Pope and G. Goldin, "Transport budgets in turbulent lifted flames of methane autoigniting in a vitiated co-flow," *Combustion and Flame*, vol. 151, p. 495–511, 2007.
- [35] P. Domingo, L. Vervisch and D. Veynante, "Large-eddy simulation of a lifted methane jet flame in a vitiated coflow," *Combustion and Flame*, vol. 152, pp. 415-432, 2008.
- [36] S. Patwardhan, S. De, K. Lakshmisha and B. Raghunandan, "CMC simulations of lifted turbulent jet flame in a vitiated coflow," *Proceedings of the Combustion Institute*, vol. 32, pp. 1705-1712, 2009.
- [37] R. Cabra, J. Chen and R. Dibble, *Vitiated Coflow Combustor Design Package*, Combustion Analysis Laboratory, University of California at Berkeley.
- [38] R. Cabra, "Turbulent Jet Flames Into a Vitiated Coflow," NASA/CR—2004-212887, 2004.
- [39] S. Turns, *An Introduction to Combustion - Concepts and Applications* 2nd Edition, Boston: McGraw Hill, 2000.
- [40] C. Vagelopoulos and F. Egolfopoulos, "Direct Experimental Determination of Laminar Flame Speeds," *Proceedings of the Combustion Institute*, vol. 27, pp. 513-519, 1998.
- [41] S. Jha, S. Fernando and S. Filip To, "Flame temperature analysis of biodiesel blends and components," *Fuel*, vol. 87, pp. 1982-1988, 2008.
- [42] W. Rasband, "ImageJ," U. S. National Institutes of Health, 1997-2014. [Online]. Available: <http://imagej.nih.gov/ij>.

- [43] D. Veynante, L. Vervisch, T. Poinso, A. Linan and G. Ruetsch, "Triple Flame Structure and Diffusion Flame Stabilization," in *Center for Turbulence Research Proceedings of the Summer Program*, 1994.
- [44] B. Dally, A. Karpetis and R. Barlow, "Structure of turbulent non-premixed jet flames in a diluted hot coflow," *Proceedings of the Combustion Institute*, vol. 29, pp. 1147-1154, 2002.
- [45] C. Arndt, R. Schießl, J. Gounder, W. Meier and M. Aigner, "Flame stabilization and auto-ignition of pulsed methane jets in a hot coflow: Influence of temperature," *Proceedings of the Combustion Institute*, vol. 34, pp. 1483-1490, 2013.
- [46] D. Goodwin, H. Moffat and R. Speth, "Cantera: An object- oriented software toolkit for chemical kinetics, thermodynamics, and transport processes," 2014. [Online]. Available: <http://www.cantera.org>.
- [47] G. Smith, D. Golden, M. Frenklach, N. Moriarty, B. Eiteneer, M. Goldenberg, C. T. Bowman, R. Hanson, S. Song, W. Gardiner Jr., V. Lissianski and Z. Qin, "GRI-Mech," [Online]. Available: http://www.me.berkeley.edu/gri_mech/.
- [48] T. Echehki and J. Chen, "Direct numerical simulation of autoignition in non-homogeneous hydrogen-air mixtures," *Combustion and Flame*, vol. 134, pp. 169-191, 2003.
- [49] P. Medwell and B. Dally, "Experimental Observation of Lifted Flames in a Heated and Diluted Coflow," *Energy & Fuels*, vol. 26, pp. 5519-5527, 2012.
- [50] C. N. Markides and E. Mastorakos, "An experimental study of hydrogen autoignition in

a turbulent co-flow of heated air," *Proceedings of the Combustion Institute*, vol. 30, pp. 883-891, 2005.